

COMPARATIVE STUDY OF LOW TEMPERATURE WATER GAS SHIFT  
REACTION OVER PARTICULATE AND MONOLITHIC CATALYSTS

by

Sevinç Tuna

B.S. in Ch.E., Yıldız Technical University, 2007

Submitted to the Institute for Graduate Studies in  
Science and Engineering in partial fulfillment of  
the requirements for the degree of  
Master of Science

Graduate Program in Chemical Engineering

Boğaziçi University

2009

*to my family*

## ACKNOWLEDGEMENTS

Firstly, I owe my deepest gratitude to my thesis advisor Prof. Zeynep İlsen Önsan for her advice, support and especially for her continuous encouragement during my MS thesis. The way of approaching and analyzing the cases in our weekly meetings were admirable. I am grateful to her for her patience. Without her guidance and persistent help this dissertation would not have been possible. It was a privilege for me to work with Prof. Zeynep İlsen Önsan.

I would also like to acknowledge my thesis co-advisor Assist. Prof. Ahmet Kerim Avcı for providing valuable insight and for his help at all times. His suggestions on different aspects were also helpful in completing my thesis. Special thanks to my thesis committee members, Prof. Ayşe Nilgün Akın, Assoc. Prof. Ramazan Yıldırım and Assist. Prof. A. Kerem Uğuz for spending their time and for contributions to my dissertation.

I am indebted to Feyza Gökalliler for her support, encouragement and friendship.

Special thanks are due to Sabriye Güven, Hacer Güneş, İlker Öztürk, Fatma Akpınar and Görkem Oğur for their enjoyable friendship and sharing their experiences with me.

Cordial thanks to Bilgi Dedeoğlu, Nurettin Bektaş and Yakup Bal for their technical assistance and friendship during my thesis. Heartfelt thanks are for Melike Gürbüz and Fatma Coşkun for their friendship and kindness to me.

I cannot end without thanking my parents, on whose constant encouragement and love I have relied throughout my life. Their wholehearted support and conviction will always inspire me. It is to them that I dedicate this work.

Financial support provided by Boğaziçi University projects 06HA501 and 08A503 and by the TÜBİTAK project 104M163 are gratefully acknowledged.

## ABSTRACT

### COMPARATIVE STUDY OF LOW TEMPERATURE WATER GAS SHIFT REACTION OVER PARTICULATE AND MONOLITHIC CATALYSTS

Low temperature water gas shift (LTWGS) performance of supported Pt-ceria catalysts was investigated over particulate and monolithic structures using both pure and mixed realistic feed compositions in the 225-300°C range. WGS reaction was carried out using three different catalysts, 1.4wt.%Pt-5wt.%CeO<sub>x</sub>/γ-Al<sub>2</sub>O<sub>3</sub> and 1.4wt.%Pt-10wt.%CeO<sub>x</sub>/γ-Al<sub>2</sub>O<sub>3</sub> in particulate form and 1.4wt.%Pt-5wt.%CeO<sub>x</sub>/γ-Al<sub>2</sub>O<sub>3</sub> in monolithic form. The experimental work involved a parametric study of the effects on CO conversion of steam to CO ratio, H<sub>2</sub> or CO<sub>2</sub> addition to the feed, simultaneous addition of H<sub>2</sub> and CO<sub>2</sub> to the feed, and cerium oxide loading. H<sub>2</sub>O/CO ratios of 1, 2, 3, 5 and 7 were used over the particulate 1.4wt.%Pt-5wt.%CeO<sub>x</sub>/γ-Al<sub>2</sub>O<sub>3</sub> catalyst at 225°C with 5 mol% CO in inert N<sub>2</sub>; increasing values of this ratio shifted the WGS reaction to the product side and increased CO conversion. H<sub>2</sub> and CO<sub>2</sub> addition effects were tested solely at the H<sub>2</sub>O/CO ratio of 3 with feed containing 5 mol% CO, 15 mol% H<sub>2</sub>O, 25 mol% H<sub>2</sub>, and 10 mol% CO<sub>2</sub> in inert N<sub>2</sub>. The existence of H<sub>2</sub> or CO<sub>2</sub> in feed suppressed CO conversion according to Le Chatelier's Principle. A more drastic decrease was observed in conversion when H<sub>2</sub> and CO<sub>2</sub> co-existed in the feed at 225°C. Experiments with both H<sub>2</sub> and CO<sub>2</sub> in the feed were repeated at 250 and 275°C to cover the temperature range of LTWGS. Catalyst performance under mixed feed conditions was also tested by doubling the ceria in particulate catalyst 1.4wt.%Pt-10wt.%CeO<sub>x</sub>/γ-Al<sub>2</sub>O<sub>3</sub>; and no significant change was observed in CO conversion. Catalytic activity of monolithic Pt-ceria catalysts were examined by loading precursor having the same metal and promoter amounts (1.4wt.%Pt-5wt.%CeO<sub>x</sub>) as the particulate catalyst onto a cordierite monolith structure; results of mixed feed experiments at 250-300°C showed that monoliths require higher temperatures for reaching the CO conversion levels of particulate catalysts with similar composition.

## ÖZET

### PARÇACIKLI VE MONOLİTİK KATALİZÖRLERDE SU GAZI GEÇİŞ REAKSİYONUNUN KARŞILAŞTIRMALI ÇALIŞMASI

Parçacıklı ve monolit yapılar üzerine yüklenmiş destekli Pt-CeO<sub>2</sub> katalizörlerinin katalizlediği düşük-sıcaklık su gazı geçiş (LTWGS) reaksiyonu 225-300°C sıcaklık aralığında, ideal ve gerçekçi girdi karışımları kullanılarak incelendi. Su gazı geçiş reaksiyonu için üç ayrı katalizör, parçacıklı 1.4wt.%Pt-5wt.%CeO<sub>x</sub>/γ-Al<sub>2</sub>O<sub>3</sub> ve 1.4wt.%Pt-10wt.%CeO<sub>x</sub>/γ-Al<sub>2</sub>O<sub>3</sub> ve monolit 1.4wt.%Pt-5wt.%CeO<sub>x</sub>/γ-Al<sub>2</sub>O<sub>3</sub>, kullanıldı. Yapılan parametrik deneysel çalışmalarda, H<sub>2</sub>O/CO oranının, girdiye H<sub>2</sub> veya CO<sub>2</sub> eklenmesinin, girdiye H<sub>2</sub> ve CO<sub>2</sub> eklenmesinin, ve katalizörün CeO<sub>2</sub> içeriğinin CO dönüşmesi üzerindeki etkileri araştırıldı. İnert N<sub>2</sub> ortamında yüzde beş mol CO içeren girdide H<sub>2</sub>O/CO oranları 1, 2, 3, 5 ve 7 olarak değiştirildi; oran yükseldikçe reaksiyonun ürün tarafına kaydığı ve CO dönüşmesinin arttığı gözlemlendi. Girdiye H<sub>2</sub> veya CO<sub>2</sub> eklenen deneylerde H<sub>2</sub>O/CO oranı 3 ve girdi bileşimi mol bazında %5 CO, %15 H<sub>2</sub>O, %25 H<sub>2</sub> veya %10 CO<sub>2</sub> ve inert N<sub>2</sub> olarak belirlendi. 225°C de girdiye H<sub>2</sub> veya CO<sub>2</sub> eklenmesi Le Chatelier ilkesine göre ileri reaksiyonu yavaşlatarak CO dönüşmesini azalttı. H<sub>2</sub> ve CO<sub>2</sub> nin birlikte eklenmesi dönüşmede çarpıcı bir düşüşe yol açtı; düşük-sıcaklık su gazı geçiş reaksiyonu için tüm sıcaklık aralığını tamamlamak amacıyla bu deneyler 250 ve 275°C de tekrarlandı. CeO<sub>2</sub> yüzdesi iki katına çıkarılarak 1.4wt.%Pt-10wt.%CeO<sub>x</sub>/γ-Al<sub>2</sub>O<sub>3</sub> parçacıklı katalizörü ile gerçekçi girdi karışımı kullanılarak yapılan ek deneyler CO dönüşmesini önemli ölçüde etkilemedi. Parçacıklı 1.4wt.%Pt-5wt.%CeO<sub>x</sub> katalizörü ile aynı miktarda metal ve katkı içeren, kordierit monolit yapı üzerine yüklenmiş Pt-CeO<sub>2</sub> monolit katalizörlerinin katalitik etkinlikleri incelendi; gerçekçi girdi karışımıyla 250-300°C sıcaklık aralığında elde edilen deney sonuçları, yüksek CO dönüşmelerine erişilebilmesi için monolitlerin aynı bileşimdeki parçacıklı katalizörlere nazaran daha yüksek sıcaklıklar gerektirdiğini gösterdi.

## TABLE OF CONTENTS

ACKNOWLEDGMENTS .....	iv
ABSTRACT.....	v
ÖZET .....	vi
LIST OF FIGURES.....	ix
LIST OF TABLES .....	xi
LIST OF SYMBOLS/ABBREVIATIONS.....	xiii
1. INTRODUCTION.....	1
2. LITERATURE SURVEY .....	3
2.1. Fuel Cells.....	3
2.2. On-Board Hydrogen Production.....	6
2.3. Water-Gas Shift Reaction.....	8
2.3.1. High Temperature Water-Gas Shift Reaction.....	9
2.3.1. Low Temperature Water-Gas Shift Reaction .....	13
2.3.1.1. Nonprecious Metal Catalysts.....	13
2.3.1.2. Precious Metal Catalysts .....	18
2.4. Water Gas Shift Catalysts .....	25
2.4.1. Particulate Catalysts .....	25
2.4.1.1. Platinum as a catalyst.....	25
2.4.1.2. Ceria as a catalyst .....	26
2.4.1.3. Alumina as a support.....	26
2.4.2. Monolithic Catalyst .....	27
3. EXPERIMENTAL WORK.....	28
3.1. Materials.....	28
3.1.1. Chemicals.....	28
3.1.2. Gases and Liquids .....	28
3.2. The Experimental System .....	29
3.2.1. Catalyst Preparation System .....	29
3.2.2. Reaction Section.....	31
3.2.3. Product Analysis Section.....	32
3.3. Catalyst Preparation.....	34

3.3.1. Incipient Wetness Impregnation Procedure.....	34
3.3.2. Wash Coating and Co-impregnation Procedure.....	35
3.3.2.1. Wash-coating with colloidal alumina solution.....	35
3.3.2.2. Co-impregnation method.....	36
3.4. Catalytic Activity Measurements .....	36
4. RESULTS AND DISCUSSION .....	38
4.1. Effect of H <sub>2</sub> O/CO Ratio .....	40
4.2. Effect of H <sub>2</sub> Addition to the Feed Stream .....	41
4.3. Effect of CO <sub>2</sub> Addition to the Feed Stream.....	43
4.4. Effect of H <sub>2</sub> and CO <sub>2</sub> Addition to the Feed Stream .....	44
5. CONCLUSIONS AND RECOMMENDATIONS.....	55
5.1. Conclusions .....	55
5.2. Recommendations.....	56
APPENDIX A : THE LIST OF EXPERIMENTS PERFORMED OVER LOW TEMPERATURE WATER GAS SHIFT REACTION .....	57
REFERENCES.....	58

## LIST OF FIGURES

Figure 3.1.	The impregnation system of particulate catalysts .....	30
Figure 3.2.	The alumina wash-coating system .....	30
Figure 3.3.	The impregnation system of monolithic catalysts .....	31
Figure 3.4.	Schematic diagram of the reactor and furnace system .....	32
Figure 4.1.	Effect of H <sub>2</sub> O/CO ratio on CO conversion at 225°C over 1.4wt.%Pt-5wt.%CeO <sub>x</sub> /γ-Al <sub>2</sub> O <sub>3</sub> .....	41
Figure 4.2.	Effect of H <sub>2</sub> in feed on CO conversion at 225°C over 1.4wt.%Pt-5wt.%CeO <sub>x</sub> /γ-Al <sub>2</sub> O <sub>3</sub> .....	42
Figure 4.3.	Effect of CO <sub>2</sub> in feed on CO conversion at 225°C over 1.4wt.%Pt-5wt.%CeO <sub>x</sub> /γAl <sub>2</sub> O <sub>3</sub> .....	44
Figure 4.4.	Effect of CO <sub>2</sub> and H <sub>2</sub> addition on CO conversion over 1.4wt.%Pt-5wt.%CeO <sub>x</sub> /γ-Al <sub>2</sub> O <sub>3</sub> using H <sub>2</sub> O/CO=3.....	45
Figure 4.5.	Effect of CO <sub>2</sub> and H <sub>2</sub> addition on CO conversion over 1.4wt.%Pt-5wt.%CeO <sub>x</sub> /γ-Al <sub>2</sub> O <sub>3</sub> using H <sub>2</sub> O/CO=5.....	46
Figure 4.6.	Effect of CO <sub>2</sub> and H <sub>2</sub> addition on CO conversion over 1.4wt.%Pt-10wt.%CeO <sub>x</sub> /γ-Al <sub>2</sub> O <sub>3</sub> using H <sub>2</sub> O/CO=5.....	48
Figure 4.7.	Effect of temperature on CO conversion over 1.4wt.%Pt-5wt.%CeO <sub>x</sub> /γ-Al <sub>2</sub> O <sub>3</sub> monolithic catalyst using pure feed and H <sub>2</sub> O/CO=3.....	49

Figure 4.8.	Effect of temperature on CO conversion over 1.4wt.%Pt-5wt.%CeO <sub>x</sub> /γ-Al <sub>2</sub> O <sub>3</sub> monolithic catalyst using mixed feed with CO <sub>2</sub> and H <sub>2</sub> at H <sub>2</sub> O/CO=3.....	50
Figure 4.9.	Effect of Pt-CeO <sub>x</sub> catalyst type on CO conversion using realistic mixed feed with CO <sub>2</sub> and H <sub>2</sub> at H <sub>2</sub> O/CO=3.....	52
Figure 4.10.	Comparison of CO conversions over 1.4wt.%Pt-5wt.%CeO <sub>x</sub> /γ-Al <sub>2</sub> O <sub>3</sub> with equilibrium data using mixed feed with CO <sub>2</sub> and H <sub>2</sub> at H <sub>2</sub> O/CO=3 (90 min time-on-stream).....	53
Figure 4.11.	Comparison of CO conversions over 1.4wt.%Pt-5wt.%CeO <sub>x</sub> /γ-Al <sub>2</sub> O <sub>3</sub> with equilibrium data using mixed feed with CO <sub>2</sub> and H <sub>2</sub> at H <sub>2</sub> O/CO=5 (90 minutes time on stream).....	53
Figure 4.12.	Comparison of CO conversions over monolithic Pt-CeO <sub>x</sub> catalyst with equilibrium data using mixed feed with CO <sub>2</sub> and H <sub>2</sub> at H <sub>2</sub> O/CO=3 (90 min time-on-stream).....	54

## LIST OF TABLES

Table 3.1.	Chemicals used in catalyst preparation .....	28
Table 3.2.	Applications and specifications of the liquids used .....	29
Table 3.3.	Applications and specifications of the gases used .....	29
Table 3.4.	Reactant and product gas analysis conditions .....	32
Table 3.5.	Reduction program for Pt-CeO <sub>x</sub> /γ-Al <sub>2</sub> O <sub>3</sub> catalysts .....	37
Table 3.6.	Reduction conditions for catalytic activity tests .....	37
Table 4.1.	Effect of H <sub>2</sub> O/CO ratio on CO conversion at 225°C over 1.4wt.%Pt-5wt.%CeO <sub>x</sub> /γ-Al <sub>2</sub> O <sub>3</sub> .....	40
Table 4.2.	Effect of product H <sub>2</sub> in the feed on CO conversion at 225°C over 1.4wt.%Pt-5wt.%CeO <sub>x</sub> /γ-Al <sub>2</sub> O <sub>3</sub> using feed with 5% CO, 15% H <sub>2</sub> O in N <sub>2</sub> .....	42
Table 4.3.	Effect of product CO <sub>2</sub> in the feed on CO conversion at 225°C over 1.4wt.%Pt-5wt.%CeO <sub>x</sub> /γ-Al <sub>2</sub> O <sub>3</sub> using feed with 5% CO, 15% H <sub>2</sub> O in N <sub>2</sub> .....	43
Table 4.4.	Effect of 25%H <sub>2</sub> and 10%CO <sub>2</sub> in the feed on CO conversion at H <sub>2</sub> O/CO=3 over 1.4wt%Pt-5wt%CeO <sub>x</sub> /γ-Al <sub>2</sub> O <sub>3</sub> .....	45
Table 4.5.	Effect of 25% H <sub>2</sub> and 10% CO <sub>2</sub> in the feed on CO conversion at H <sub>2</sub> O/CO=5 over 1.4wt.%Pt-5wt.%CeO <sub>x</sub> /γ-Al <sub>2</sub> O <sub>3</sub> .....	46

Table 4.6.	Effect of 25% H <sub>2</sub> and 10% CO <sub>2</sub> in the feed on CO conversion at H <sub>2</sub> O/CO=5 over 1.4wt.%Pt-10wt.%CeO <sub>x</sub> /γ-Al <sub>2</sub> O <sub>3</sub> .....	47
Table 4.7.	CO conversion over 1.4wt.%Pt-5wt.%CeO <sub>x</sub> /γ-Al <sub>2</sub> O <sub>3</sub> monolithic catalyst with pure feed using H <sub>2</sub> O/CO=3.....	49
Table 4.8.	CO conversion over 1.4wt.%Pt-5wt.%CeO <sub>x</sub> /γ-Al <sub>2</sub> O <sub>3</sub> monolithic catalyst using mixed feed with CO <sub>2</sub> and H <sub>2</sub> at H <sub>2</sub> O/CO=3.....	50
Table 4.9.	Comparison of CO conversions over particulate and monolithic Pt-CeO <sub>x</sub> catalysts using mixed feed with CO <sub>2</sub> and H <sub>2</sub> at H <sub>2</sub> O/CO=3.....	52

**LIST OF SYMBOLS/ABBREVIATIONS**

R	Ideal Gas Constant
T	Temperature
$\Delta H$	Enthalpy of the reaction
$\Delta G_i$	Gibbs free energy of reaction
AFC	Alkaline Fuel Cell
ATR	Autothermal Reforming
BET	Branauer Emmett Teller
BOS	Birleşik Oksijen Sanayi
CA	Citric Acid
CP	Co-Precipitation
cpsi	cells per square inch
EG	Ethylene Glycol
FC	Fuel Cell
GDL	Gas Diffusion Layer
HTS	High Temperature Shift
HT-WGS	High Temperature Water Gas Shift
ID	Initial Diameter
LTS	Low Temperature Shift
LT-WGS	Low Temperature Water Gas Shift
MEA	Membrane Electrode Assembly
MCFC	Molten Carbonate Fuel Cell
PAFC	Phosphoric Acid Fuel Cell
PEM	Proton Exchange Membrane
PEMFC	Proton Exchange Membrane Fuel Cell
POX	Partial Oxidation
PROX	Preferential Oxidation
R	Rutile
SMSI	Strong Metal Support Interactions

SOFC	Solid Oxide Fuel Cell
SR	Steam Reforming
TCD	Thermal Conductivity Detector
THF	Tetra Hydro Furan
TOF	Turn Over Frequency
TOX	Total Oxidation
TPR	Temperature Programmed Reduction
WGS	Water Gas Shift
WGSR	Water Gas Shift Reaction
WHSV	Weight Hourly Space Velocity
YSZ	Yttria Stabilized Zirconia

## 1. INTRODUCTION

Investigations of highly efficient, cleaner devices and utilization systems pave the way for the development of the sustainable energy systems (Song, 2002). A variety of fuel cells have already been developed, but the proton exchange membrane fuel cells (PEMFC), which are considered as energy efficient devices, are promising candidates for automotive applications to lower the fuel consumption and to reduce harmful emissions (Boettner and Moran, 2004). Pure hydrogen is a superior PEMFC feed but its distribution and storage difficulties present serious disadvantages to its direct use for fuel cell propulsion systems (Brown, 2001). Therefore, on-board hydrogen production from a suitable hydrocarbon source appears to be a practical option (Patel and Pant, 2006). Fuel processors can convert most of the available hydrocarbon fuels into hydrogen on-board a vehicle.

In a fuel processor, three catalytic processes are in series for the production of hydrogen: (i) autothermal reforming of hydrocarbon for H<sub>2</sub> production (ATR), (ii) water-gas shift (WGS) reaction and (iii) selective catalytic oxidation of carbon monoxide (PROX). The composition of reformer outlet includes approximately 10 mol per cent carbon monoxide which should be removed as it is both a pollutant and a poison for the platinum electrodes of the fuel cell (Goguet *et al.*, 2004). WGS converter is added after the reformer to convert CO to meet this goal. The WGS reaction reduces the CO level to 0.5-1 volume per cent and is generally followed by an additional selective CO oxidation stage to reduce the CO level to about 10 ppm (Zalc *et al.*, 2002).

Industrially, the WGS reaction is carried out in two stages with different temperature regions. The high-temperature shift (HTS) is at 350-450°C and catalysts are based on Fe-Cr oxides. The low-temperature shift (LTS) is usually between 200-260°C and typical catalysts are based on Cu/ZnO/Al<sub>2</sub>O<sub>3</sub> (Zalc and Löffler, 2002). Copper-ceria catalysts among the non-precious metal/support systems are the alternatives to the commercial copper-zinc oxide low-temperature water-gas shift catalysts. The preparation method affects the activity of the catalysts directly. Among methods such as impregnation, precipitation, sol-gel and ion-exchange, those more suitable for the preparation of copper-ceria catalysts are precipitation and impregnation (Zerva and Philippopoulos, 2006).

Although Cu-based catalysts for low-temperature water-gas shift reaction have long been used, they have strong drawbacks which make them inappropriate for fuel cells. The disadvantages of copper-based catalysts have been overcome by the use of precious metal-based systems, although cost is always an important factor. Promotion by a noble metal enhances the reducibility of ceria and assists the formation of surface oxygen vacancies. Pt/CeO<sub>2</sub> catalyst seems to be the most promising among those catalysts and is generally prepared by the impregnation method (Farias *et al.*, 2007).

The objective of this study was to investigate the low-temperature water-gas shift performance of Pt-ceria catalysts supported on particulate and monolithic structures using both pure and mixed realistic feed compositions in the 225-300°C range. The particulate catalysts studied were divided into two groups according to their cerium oxide loading, 1.4wt.%Pt-5wt.%CeO<sub>x</sub>/γ-Al<sub>2</sub>O<sub>3</sub> and 1.4wt.%Pt-10wt.%CeO<sub>x</sub>/γ-Al<sub>2</sub>O<sub>3</sub> which were prepared by the sequential impregnation method whereas co-impregnation was used for preparing alumina wash-coated monoliths with 1.4wt.%Pt-5wt.%CeO<sub>x</sub> loading. Catalytic activity tests were conducted in a microreactor flow system run at atmospheric pressure at 225, 250, 275 and 300°C. The effects of the H<sub>2</sub>O/CO ratio, H<sub>2</sub> or CO<sub>2</sub> addition to the feed, and the co-existence of H<sub>2</sub> and CO<sub>2</sub> in the feed were studied with a view to compare particulate and monolithic catalysts of similar composition.

Section 2 includes a literature survey on fuel cells, on-board hydrogen production, characteristics of high and low-temperature water-gas shift reactions and catalysts used for these reactions. In Section 3, the experimental procedures used for the catalyst preparation and the activity tests are presented. Section 4 focuses on the discussion of the experimental results that were obtained; the conclusions of this study and recommendations for future work are given in Section 5.

## 2. LITERATURE SURVEY

### 2.1. Fuel Cells

An awareness of global climate-warming issues accompanied by the economic and strategic issues associated with fossil fuels provides a strong motivation for society to find and develop replacement technologies for the supply of energy (Gerbec *et. al.*, 2008).

Fuel cell systems have received increased attention in recent years as an available alternative for clean energy generation (Cipiti *et. al.*, 2008). Fuel cells (FCs) are electrochemical devices that directly convert the Gibbs energy of reaction of a fuel with an oxidant into electricity (Feng *et. al.*, 2004) without combustion. Unlike thermal engines, their thermodynamic efficiency is not limited by that of a Carnot cycle and is in fact generally much higher than that of thermal engines. Although other factors limit the efficiency of the present-generation fuel cells to 40–50%, this is still two to three times that of the internal combustion engine of a typical vehicle. The most of fuel cells are fed by pure hydrogen or hydrogen-rich gas mixtures produced by catalytic conversion of hydrocarbons (Badmaev and Snytnikov, 2008). Heat and water vapor are the only by-products (Li *et. al.*, 2000).

The absence of a hydrogen refueling infrastructure and the problems concerning hydrogen storage, have led to the development of fuel processors able to convert available fuels (hydrocarbons and/or alcohols) into hydrogen rich reformat gas ( $H_2+CO$ ) (Joensen and Rosstrup-Nielsen, 2002). These fuel processors will contain catalytic reactors that carry out one or more reactions between the fuel, steam, and/or oxygen (Krumpelt *et. al.*, 2002). The key requirements for a fuel processor include rapid start-up, good dynamic-response to change in hydrogen demand, high fuel conversion, small size and weight, simple design (construction and operation), stable performance for repeated start-up and shut-down cycles, maximum thermal integration, low cost and maintenance, high reliability and safety (Ahmed and Krumpelt, 2001).

Fuel cells can be grouped by the type of electrolyte they use, namely :

Alkaline fuel cells (AFC) use concentrated (85wt.%) KOH as the electrolyte for high temperature operation (250°C) and less concentrated (35–50wt.%) for lower temperature operation (<120°C). The electrolyte is retained in a matrix (usually asbestos), and a wide range of electrocatalysts can be used (such as Ni, Ag, metal oxides and noble metals). This fuel cell is intolerant to CO<sub>2</sub> present in either fuel or oxidant. Alkaline fuel cells have been used in the space program (Apollo and Space Shuttle) since 1960s (Barbir, 2005).

Polymer electrolyte membrane or proton exchange membrane fuel cells (PEMFC) use a thin ( $\leq 50$   $\mu\text{m}$ ) proton conductive polymer membrane (such as perfluorosulfonated acid polymer) as the electrolyte. The catalyst is typically platinum supported on carbon with loadings of about 0.3 mg/cm<sup>2</sup>, or if the hydrogen feed contains minute amounts of CO, Pt-Ru alloys are used. Operating temperature is typically between 60 and 80°C. PEM fuel cells are a serious candidate for automotive applications, but also for small-scale distributed stationary power generation, and for portable power applications as well (Barbir, 2005).

Phosphoric acid fuel cells (PAFC) use concentrated phosphoric acid (~100%) as the electrolyte. The matrix used to retain the acid is usually SiC, and the electrocatalyst in both the anode and the cathode is platinum. Operating temperature is typically between 150 and 220°C. phosphoric acid fuel cells are already semicommercially available in container packages (200 Kw), for stationary electricity generation (UTC fuel cells). Hundreds of units have been installed all over the world (Barbir, 2005).

Molten carbonate fuel cells (MCFC) have the electrolyte composed of a combination of alkali (Li, Na, K) carbonates, which is retained in a ceramic matrix of LiAlO<sub>2</sub>. Operating temperatures are between molten salt, with carbonate ions providing ionic conduction. At such high operating temperatures, noble metal catalysts are typically not required. These fuel cells are in the precommercial/demonstration stage for stationary power generation (Barbir, 2005).

Solid oxide fuel cells (SOFC) use a solid, nonporous metal oxide, usually Y<sub>2</sub>O<sub>3</sub>-stabilized ZrO<sub>2</sub> (YSZ) as the electrolyte. These cells operate at 800 to 1000°C where ionic conduction by oxygen ions takes place. Similar to MCFC, these fuel cells are in the

precommercial/demonstration stage for stationary power generation, although smaller units are being developed for portable power and auxiliary power in automobiles (Barbir, 2005).

Among several types of FCs, the polymer electrolyte membrane (PEM) fuel cell is the most popular for transportation and portable applications. The polymer electrolyte fuel cell (PEFC) fuelled by hydrogen appears to be the key option for both transport and small scale combined heat and power applications, due to its compactness, modularity, higher conversion efficiencies, lightweight, durability, high power density and rapid power demands and low emissions of noise and pollutants (Feng *et al.*, 2004). Hydrogen delivery for these applications must be high density (energy/weight $>1$ ) (Buxbaum and Lei, 2003) and able to follow a varying load with only a few seconds lag at most. Furthermore, the hydrogen must be delivered relatively pure, containing few tens of ppm CO. (Brunetti *et al.*, 2008).

The crucial part of the PEMFC is the membrane electrode assembly (MEA) which consists of a proton exchange membrane with a layer of catalyst on both sides and a gas diffusion layer (GDL) in contact with each of the catalyst layers. The macroporous layer of the GDL is either carbon paper or woven carbon cloth and it serves as a current collector, a physical substrate for the catalyst layer and an elastic component of the MEA. GDL is one of the critical components of a fuel cell that has the ability to influence the H<sub>2</sub>/air system as its basic functions are transportation of the reactant gas from flow channels to catalyst layer effectively, draining out liquid water from catalyst layer to flow channels, conducting electrons with low resistance and keeping the membrane in wet condition at low humidity (Cindrella *et al.*, 2009).

Carbon monoxide present in the fuel gas deteriorates the Pt electrode of PEMFC and degrades the cell performance and it is known as CO poisoning (Iida and Igarashi, 2006). The CO competes with the adsorption of hydrogen on the active sites of platinum at normal anode operating potentials. CO reacts with the hydroxyl species that are adsorbed on the platinum surface to form CO<sub>2</sub>. This case results, however, in a serious loss of efficiency and is not practical (Adams *et al.*, 2005).

Hydrogen can be stored in tanks as compressed or liquefied H<sub>2</sub>, in hydrogen storage alloys, and on activated carbon or nanoscale materials such as carbon nanotubes. Unfortunately, their volumetric and gravimetric efficiency are still too low to meet the requirements, whereas *in situ* or on-board hydrogen generation is becoming increasingly important as a potential route to supply hydrogen for the PEM fuel cell (Xua *et. al.*, 2008).

## 2.2. On Board Hydrogen Production

A number of different types of fuels have been considered for hydrogen production in fuel processors (Qi *et. al.*, 2007). Natural gas, which is mainly methane, is a very stable, symmetrical molecule. Its C–H bonds are strong (425 kJ/mol) and it contains no functional group, magnetic moment or polar distribution to facilitate chemical attacks. Activation of methane by splitting of the C–H bond will require high temperatures and/or the use of oxidations agents. Catalysis will have to play an important role in most processes for methane conversion (Holmen, 2009). It also accounts for almost half the feedstock used for H<sub>2</sub> production in the world and has the lowest greenhouse effect in terms of CO<sub>2</sub> emissions, in addition to high conversion efficiency and a wide transportation network (Avcı *et. al.*, 2002).

The major chemical processes used for hydrogen production from hydrocarbon fuels for PEMFC applications are steam reforming, direct partial oxidation, and autothermal reforming (Ahmed and Krumpelt, 2001).

Steam reforming (SR) reaction is typically carried out at 800–900°C and 15–30 bar and generally carried out with reactions 1 and 2. (Solieman *et. al.*, 2009). In some cases the CO<sub>2</sub> may replace the water in reaction (3) and lead to a different ratio of H<sub>2</sub>:CO, via dry reforming of methane (Lucrédio *et. al.*, 2009).



Catalytic partial oxidation (POX) is an alternative process to steam reforming, the industrial process for production of synthesis gas from natural gas. Heat required to support the endothermic steam reforming reaction is provided by partial oxidation (POX) resulting in a lower overall temperature (Chan and Wang, 2000) and (POX) is a more energy efficient and less expensive process than steam reforming (Shamsi, 2009). The POX process is capable of producing syngas with a H<sub>2</sub>/CO ratio of about 2, which makes it favorable for methanol and hydrocarbon synthesis (Sun *et. al.*, 2005).



Autothermal reforming (ATR) is the most promising reforming technology for fuel cell systems, since the combination of catalytic TOX, SR, and high-temperature WGS reactions allows the design of more compact adiabatic reactors with low pressure drop (Farrauto *et. al.*, 2003). ATR combines thermal effects from both SR and POX reforming so that the heat required to support the endothermic steam reforming reaction is provided by oxidation reactions, resulting in a lower overall temperature (Chan and Wang, 2000). Also since ATR generates heat in situ, it does not require an external burner or heat exchangers like SR (Reese *et. al.*, 2009). Inlet temperature, steam-to carbon, and oxygen-to-carbon ratios in the feed as well as reactor pressure are the independent variables of the ATR reactor, while the exit temperature and fuel conversion are the dependent variables. The parameter to be maximized is the H<sub>2</sub> yield (mol H<sub>2</sub> produced/mol fuel converted) (Hagh, 2003).



The water-gas shift (WGS) reaction, the second step in the hydrogen production following autothermal reforming, eliminates most of the CO and produces more hydrogen. The gas from the reformer and water-gas shift reactor contains H<sub>2</sub>, CO<sub>2</sub>, H<sub>2</sub>O, traces of unconverted fuel and 0.5-1 volume per cent CO, thus improving H<sub>2</sub> yield (Sedmak *et al.*, 2004). It is imperative to lower the remaining carbon monoxide levels less than 50 ppm as indicated by the poisoning limit of PEM fuel cell electrodes at the third and final cleanup step by preferential oxidation (PROX). The PROX reaction is the selective catalytic oxidation of CO (CO + ½ O<sub>2</sub> → CO<sub>2</sub> ΔH = -283.2 kJ/mol). In order to achieve low CO

concentration, the PROX reactor is placed between the shift reactor and the fuel cell anode (Cheekatamarla *et al.*, 2005). Selectivity is a serious issue in the PROX unit, because the oxidation of hydrogen leads to reduce process efficiency and increased water management issues. Therefore, the reforming, water-gas shift and preferential oxidation reactors represent a large fraction of the volume and cost and pose the greatest technical challenges (Zalc and Löffler, 2002).

### 2.3. Water Gas Shift Reaction

Basically, the water-gas shift (WGS) reaction is implemented by conversion of both carbon monoxide and water into hydrogen and carbon dioxide (Thinon *et al.*, 2008).



where  $\Delta H = -41.2 \text{ kJ.mol}^{-1}$  and  $\Delta G = -28.6 \text{ kJ.mol}^{-1}$  (Wen *et al.*, 2007; and Li *et al.*, 2000). The WGS reaction is exothermic, so that heat management is a critical component of any fuel processing strategy employing WGS reactors (Scott *et al.*, 2001).

The function of the WGS reaction is to reduce the carbon monoxide concentration (Scott *et al.*, 2001) because Pt electrode on PEMFC is not tolerant to fuels containing CO more than 20 ppm (Gorte and Zhao, 2005). The exit product stream of the SR-based reformer contains up to 12% CO, while that of an ATR-based reformer contains 6%-8% CO (Farrauto *et al.*, 2003). WGS converters are therefore used to reduce the CO content first to 3%-4% by high temperature WGS and then to 0.5%-1% by low temperature WGS (Trimm, 2005; Giroux *et al.*, 2005). If the reformer effluent contains less than ~5% CO, a single low-temperature WGS reactor may be sufficient for attaining the maximum CO content of  $\leq 2\%$  in the WGS exit (Avcı *et al.*, 2001; Semelsberger *et al.*, 2004). These facts explain why the water-gas shift (WGS) reactor is a critical component of the fuel processor (Scott *et al.*, 2001).

The CO content of water-gas shift reactor off-gas should not exceed 1 vol%. Lower values are preferred but they increase the size of the WGS reactor. To limit the reactor size, water-gas shift is usually performed in two stages with intermediate cooling preferably by

water injection (Twigg, 1989). Therefore, two WGS reactors are typically employed in a fuel processing system: one at high temperatures for initial CO conversion, and a second at low temperatures to take advantage of lower equilibrium CO contents (Scott *et al.*, 2001).

Existing applications of WGS reaction typically combine a high-temperature shift (HTS) stage governed by Arrhenius-like reaction kinetics (catalysis rates increase at higher temperatures) and a low-temperature shift (LTS) stage governed by thermodynamics (equilibrium CO contents are lower at low temperatures) (Scott *et al.*, 2001).

### 2.3.1. High Temperature Water Gas Shift Reaction

The high-temperature shift (HTS) reaction is industrially performed at 320–450°C (Natesakhawat *et al.*, 2006), using iron oxide, as well as chromium oxide (Costa *et al.*, 2002).

For the high temperature catalyst, Fe-Cr oxide has demonstrated high WGS activity and excellent thermostability, probably because the Cr promoter acts as a structural stabilizer and/or a structure promoter (Rhodes *et al.*, 2002), since in the absence of chromium oxide, the effective lifetime of the catalyst is severely restricted due to rapid thermal sintering (Keiski and Salmi, 1992). The role of chromia is mainly to stabilise the material, although recent studies have shown that it can also catalyze the reaction, but in a lower extension than iron oxide (Martos *et al.*, 2008).

There are several attempts to explain the promoter effect of chromia. According to Rangel and co-workers (1995), chromia forms a solid solution in  $\text{Fe}_3\text{O}_4$  and that  $\text{Cr}^{3+}$  displaces equal amounts of  $\text{Fe}^{2+}$  and  $\text{Fe}^{3+}$  from the octahedral sites and the displaced  $\text{Fe}^{2+}$  was consequently located in the tetrahedral site. Similarly, Kappen *et al.* (2001) investigated the state of the Cu promoter (0.17–1.5wt.%) in Fe–Cr catalysts and found that Cu was in the metallic phase under the WGS reaction conditions. However, it reoxidized easily when exposed to the atmosphere.

Although Fe-Cr catalyst seems to be attractive for high temperature water gas shift reaction, there are some disadvantages including both metallic iron formation and

environmental handling difficulties of chromium. Fe-Cr catalysts are often commercialized as hematite ( $\alpha$ -Fe<sub>2</sub>O<sub>3</sub>) and are reduced in situ to produce magnetite (Fe<sub>3</sub>O<sub>4</sub>) which is found to be the active phase (Bohlbro, 1969). This reaction is highly exothermic and should be controlled to avoid the production of metallic iron, which may catalyze undesirable reactions such as Fischer–Tropsch synthesis (Lloyd *et al.*, 1996). In industrial processes, large amounts of steam are used to inhibit the metallic iron formation. However, this implies high operational costs and the development of catalysts in the active phase is much needed (Costa *et al.*, 2002).

Another disadvantage for the use of FeCr catalyst is that commercial iron-based WGS catalysts with as high as 8–14wt.% Cr promoter generally contain about 2wt.% Cr<sup>6+</sup> compound, which is highly toxic to humans and environment during its manufacture and deposition (Ladebeck and Kochloefl, 1995). However, due to the environmental restrictions concerning the discarding of chromium compounds, the search for less toxic catalysts is much needed (Costa *et al.*, 2002). Thus, it has drawn considerable attention to study Cr-free iron-based WGS catalysts in past years (Liu *et al.*, 2005).

It is possible to prepare a Cr-free iron-based WGS catalyst that is to maintain catalyst activity and thermostability (Liu *et al.*, 2005) of the iron-catalyst by correcting with crystal structure, such as  $\alpha$ -Fe<sub>2</sub>O<sub>3</sub> and  $\gamma$ -Fe<sub>2</sub>O<sub>3</sub> (Kundu *et al.*, 1988). The crystal of  $\gamma$ -Fe<sub>2</sub>O<sub>3</sub> generally possesses an imperfect cubic spinel structure, which is different from that of  $\alpha$ -Fe<sub>2</sub>O<sub>3</sub>, hexagonal structure (Liu *et al.*, 2005). The imperfect spinel of  $\gamma$ -Fe<sub>2</sub>O<sub>3</sub> allows promoters such as Cr or Ce to be incorporated into vacant sites in the  $\gamma$ -Fe<sub>2</sub>O<sub>3</sub>, resulting in less sintering of active phase in the catalysts consisting of  $\gamma$ -Fe<sub>2</sub>O<sub>3</sub> than those containing  $\alpha$ -Fe<sub>2</sub>O<sub>3</sub> under identical operating conditions (Kundu *et al.*, 1988). To this end, it is very important to form as much  $\gamma$ -Fe<sub>2</sub>O<sub>3</sub> as possible during preparation of Cr-free iron-based WGS catalyst (Liu *et al.*, 2005).

The replacement of chromium by molybdenum in magnetite-based catalysts prepared by both oxidation–precipitation and wet impregnation was studied by Martos and colleagues (2008). During the preparation of FeMo catalysts, wet impregnation method produced materials composed by  $\gamma$ -Fe<sub>2</sub>O<sub>3</sub> with lower reducibility which in turn their activation to be more difficult. When oxidation–precipitation was used, molybdenum was

totally incorporated into the magnetite lattice for all the range of composition studied. This gave larger crystallite sizes and lower specific surface areas than those of FeCr catalysts, obtaining materials with high thermal stability of the active phase. The properties of molybdenum and copper-doped catalysts synthesized by oxidation–precipitation were similar to that of FeCrCu materials in terms of catalytic activity, product distribution and thermal stability.

Costa *et al.* (2002) examined the use of thorium instead of chromium in iron- and copper-based catalysts for the HTS reaction. It was found that the thorium and copper-doped catalyst was more active than the commercial Fe–Cr–Cu catalyst using  $H_2O/CO=0.6$  at  $370^\circ C$ . Its high activity was attributed to an increase in surface area by thorium. They stated that in thorium- and copper-doped magnetite catalyst, copper acts as a structural promoter whereas thorium prevents sintering and the production of metallic iron which can catalyze undesirable reactions. They also established that the most active catalyst was obtained when both thorium and copper are present in the solid which is more active and selective than a chromium- and copper-doped commercial catalyst.

Adding both aluminum and copper for preparing Cr-free Fe-based HTS catalysts was investigated by Natesakhawat *et al.* (2006) using two-step CP–impregnation and one-step CP methods. They found that the addition of aluminum stabilizes the magnetite phase by retarding its further reduction to FeO or metallic iron. Aluminum is a promising chromium replacement to act as a textural promoter for iron-based water gas shift catalyst. They also revealed that the promotion of Cu species is affected by preparation methods significantly. With two-step preparation, the major portion of Cu species is on the iron oxide surface, which is reduced to metallic Cu after reduction. The main promotion of the Cu species in this preparation is to provide additional active sites. With increasing reaction temperature, the promotional effect of Cu decays because of sintering of the metallic Cu, the same phenomenon observed in low temperature water gas shift catalysts. With one-step preparation, the major portion of Cu species coprecipitates with iron oxide. This Cu species is also reduced to metallic Cu at reaction conditions to provide additional active sites. However, this Cu species is not as prone to sintering as the surface Cu due to the spacer function of the iron oxide. They also stated that unavailability for reduction of some Cu species was mainly attributed to the incorporation of Cu into the iron oxide matrix.

Decreasing the chromium content by adding suitable compounds instead of preparing Cr-free catalysts is another option for alleviating the toxicity issue. Rhodes *et al.* (2002) examined the promotion of Fe–Cr catalysts with 2wt.% B, Cu, Ba, Pb, Hg, and Ag. A beneficial effect of adding Hg, Ag, or Ba was observed between 350 and 440°C. This could be due to their different ionic sizes compared to that of Fe<sup>2+</sup>, influencing the electronic structure of the active Fe<sup>3+</sup> center. Despite its high WGS activity, it is unlikely that the toxic Hg-promoted catalyst will be considered as a commercial HTS catalyst.

Araújo and Rangel (2000) investigated the catalytic performance of Al-doped Fe-based catalyst with small amounts of copper (Cu≈3wt.%), prepared by coprecipitation–impregnation method, in the HTS reaction. This sample easily produces the active phase, and has similar catalytic properties, as compared to the chromium and copper-doped commercial one. In addition, it can work at low steam to process gas ratio (S/G =0.4) as well as at low temperatures, leading to energy save and also it has the advantage of being discarded without any damage to the environment.

In recent years, studies show that CeO<sub>2</sub> is promising for the high WGS reaction (Wang *et al.*, 2002; Qi and Flytzani-Stephanopoulos, 2004). It was reported that the Ce promoter increases the reducibility of metals and inhibits metal sintering (Qi and Flytzani-Stephanopoulos, 2004). Most recently, some groups reported that addition of CeO<sub>2</sub> to Fe–Cr- and Cr-free Fe- and Cu-based WGS catalysts effectively modified catalyst performance (Hu *et al.*, 2000; Qi and Flytzani-Stephanopoulos, 2004).

Catalysts structured as bimetallic phase is another issue for increasing the WGS activity. In the study of Hua and co-workers (2005), the supported iron-based catalyst without adding promoters of Ru and lanthanum oxide did not show catalytic activity below 300°C. Catalytic activity of 0.4wt.%Ru-14wt.%Fe-MgAl<sub>2</sub>O<sub>4</sub> catalyst went up to 93% CO conversion (?) when the reaction temperature reached 400°C. They claimed that there were two advantages of using the Ru colloid as the promoter compared to impregnation of the catalyst with aqueous RuCl<sub>3</sub> solution. Firstly, the chlorine ions, which were believed to be harmful to the WGS reaction, were removed from the colloidal solution through dialysis. Secondly, the size of the metal clusters could be controlled in the preparation process. Introducing La<sub>2</sub>O<sub>3</sub> to the catalyst further increased catalytic activity.

### 2.3.2. Low Temperature Water Gas Shift Reaction

The low-temperature shift (LT-WGS) reactor operates at temperatures between 200 and 260°C to take advantage of the shift of the equilibrium to lower CO concentrations at lower temperatures (Leppelt *et al.*, 2006). Commercial catalysts used in the LT-WGS process usually consists of different combinations of CuO, ZnO and Al<sub>2</sub>O<sub>3</sub> components. (Ruettinger *et al.*, 2003).

2.3.2.1. Nonprecious Metal Catalysts. The LTWGS catalysts commonly used are Cu/ZnO/Al<sub>2</sub>O<sub>3</sub> or precious metal-based catalysts (Natesakhawat *et al.*, 2006) in the temperature range of 200 and 250°C. (Tanaka *et al.*, 2003b). Morphological characteristics such as crystallinity and surface area of the copper based catalysts are the critical parameters influencing activity. Utaka *et al.* (2000) have applied Cu/ZnO/Al<sub>2</sub>O<sub>3</sub> catalyst prepared by co-precipitation (CP) for catalytic removal of CO by oxygen assisted WGS reaction. They showed that the activity of the catalyst depends on the surface area and crystallinity. The BET surface area of the catalysts decreased with a rise in calcination temperature. The catalyst calcined at 500 and 700°C demonstrated efficient activities for CO removal at 150 and 200°C; then it attained equilibrium conversion at 250°C or higher temperatures. They also reported that the CO conversion is dependent on space velocity and that thermodynamic equilibrium is achieved at a low space velocity. Since CO removal approaches thermodynamic equilibrium at low space velocity, highly active catalysts are needed to achieve efficient removal of CO in PEMFC applications.

Guo and colleagues (2009) examined the WGS performances of Cu/ZnO and Cu/ZnO/Al<sub>2</sub>O<sub>3</sub> catalysts in shut-down/start-up operation. They found that The Cu/ZnO catalyst showed comparable activity to the Cu/ZnO/Al<sub>2</sub>O<sub>3</sub> catalyst but better stability in shut-down/start-up cycles. They discussed that superior stability of the Cu/ZnO catalyst arose from lack of alumina that is responsible for the formation of the carbonate species and deactivation of the Cu/ZnO/Al<sub>2</sub>O<sub>3</sub> catalyst was mainly attributed to the loss of active sites due to the formation of carbonate species rather than the sintering of Cu crystallites.

Increasing the activity by adding of promoters over the copper catalyst is an another issue for improving the catalytic activity. Low-temperature water-gas shift reaction over

Mn-promoted Cu/Al<sub>2</sub>O<sub>3</sub> catalysts was conducted by Yeragi and co-workers (2006). In this study, copper was loaded on alumina by co-precipitation technique and then impregnated with manganese nitrate solutions. Experiments were conducted with five different catalysts having varying Mn content in the range of 1.8–10.9 wt.%. The CO conversion increased first with Mn concentration in the catalyst until it reached a maximum at 8.55wt.% loading and then decreased for higher loadings of Mn. The decrease in CO conversion was said to be due to the decrease in copper surface area at higher copper loadings. Various W/F<sub>CO</sub> ratios ranging from 2.5 to 16 h were also tested at a temperature of 240°C. CO conversion increased as the feed contact time was increased. CO conversion did not show a significant increase beyond a W/F<sub>CO</sub> ratio of 6 h, and a plateau was reached.

Optimum amount of additives is a key factor for reaching high conversions, since excess loadings cause aggregation of Cu particles and forming of various crystalline phases. A parametric study was implemented by Tanaka and colleagues (2003a) to find the best composition (Cu/Mn ratio) and the preparation conditions (calcination temperature) of CuMn catalyst. The optimal calcination temperature of Cu–Mn spinel oxide was estimated to be 900°C for WGS activity. Molar ratio of Cu to Mn was varied from 1/8 to 2/1 at a fixed calcination temperature of 900°C and experiments were performed in the temperature range of 200–250°C. The optimum Cu/Mn ratio was determined to be 1/2 due to the fact that excess Cu loading initiated Cu aggregation during reduction of various crystalline phases to Cu and MnO, which accompanied the decrease in CO conversion. Cu/Mn:1/2 catalyst calcined at 900°C was the optimum catalyst considered for WGS activity (Tanaka *et al.*, 2003b). In parallel with a previous study, CuMn<sub>2</sub>O<sub>4</sub> composed of Cu<sub>1.5</sub>Mn<sub>1.5</sub>O<sub>4</sub> and Mn<sub>2</sub>O<sub>3</sub> phases exhibited excellent WGS activity over 225°C which was comparable to coprecipitated Cu/ZnO/Al<sub>2</sub>O<sub>3</sub>. High-temperature reduction treatment of CuMn<sub>2</sub>O<sub>4</sub> led to aggregation of Cu and catalyst deactivation. The catalyst showed high and stable WGS activity for 24 h in the durability test.

Cu–Mn spinel catalysts, prepared by coprecipitation with NH<sub>3</sub> (Tanaka *et al.*, 2003b), are likely to contain inhomogeneity due to formation of copper ammine complex [Cu(NH<sub>3</sub>)<sub>4</sub>]<sup>2+</sup>. Thus, further enhancement in the WGS activity of the Cu–Mn spinel catalyst can be expected by employing alternative preparation methods that facilitate homogeneous mixing of components (Tanaka *et al.*, 2005).

Iron addition effect on Cu–Mn oxide over WGS activity was investigated by Tanaka *et. al.* (2005). The Cu–Mn–Fe catalyst was prepared by the citric acid method. Partial substitution of Fe enhanced the catalytic activity of the Cu–Mn catalyst. The Mn/Fe ratio influenced reducibility of copper oxide after reduction of spinel phases. Fe-rich Cu–Mn–Fe samples possess smaller Cu particles in smaller amounts than Mn rich catalysts, and optimized Cu/Mn/Fe ratio was 1:1:1 in terms of catalytic activity.

In the study of Nagai *et. al.* (2006) the WGS reaction over nickel–molybdenum (Ni–Mo) carbide catalysts was investigated at 183°C. Nickel–molybdenum (Ni–Mo) carbide catalysts ( $\text{Ni}_1\text{Mo}_{1-x}\text{O}_y$ ) were prepared by the calcination of a mechanical mixture of nickel and molybdenum precursors and then carburized with a gas mixture of 20%  $\text{CH}_4/\text{H}_2$  in the temperature region of 550-650°C. The results indicated that the addition of nickel to the Mo precursor suppressed catalyst deactivation and enhanced catalytic activity.  $\text{Ni}_{0.25}\text{Mo}_{0.75}$  catalyst carburized at 550°C ( $\text{Ni}_{0.25}\text{Mo}_{0.75}\text{C-873}$ ) exhibited the highest activity among the catalysts studied at 183°C. The promotion of the WGS reaction activity was due to the formation of Ni–Mo oxycarbide.

The catalyst preparation procedure mentioned above was also applied to the cobalt–molybdenum ( $\text{Co}_x\text{Mo}_{1-x}$ ) oxides by Nagai and Matsuda (2006).  $\text{Co}_{0.5}\text{Mo}_{0.5}$  carburized at 550°C was found to be the most active among Co–Mo carbide catalysts. The incomplete carburization of the Co–Mo oxide formed amorphous Co–Mo oxycarbide, leading to a high activity for the LT-WGS reaction. Thus they revealed that the reactivity of both Ni–Mo and Co–Mo carbide catalysts in WGS reaction was very sensitive to carburizing temperature, leading to the creation of various carbide species, such as each or both oxycarbides and carbides of cobalt, nickel and molybdenum.

The presence of dopants affects reduction properties of  $\text{CuO}/\text{CeO}_2$ . The effects of dopants over  $\text{CuO}/\text{CeO}_2$  catalyst can be outlined as follows: increment of BET surface area and total pore volume, inhibitive effect over the growth of ceria and favoring of the production of smaller particles (Tabakova *et. al.*, 2007).

The study of Tabakova *et. al.* (2007), presents the role of additives (samaria, lanthana, zirconia, and zinc oxide) to ceria as a support of copper catalysts for LT-WGS.

Among the CuO/doped-CeO<sub>2</sub> catalysts prepared by urea-nitrate combustion method and tested in the temperature range of 150-350°C, Sm- and Zn-doped catalysts showed better activity which has been attributed to various factors, including increased BET surface area and total pore volume, decreased ceria particle size and enhanced reducibility. Addition of zirconia and lanthana caused the opposite effect. All additives inhibited crystal growth of ceria and favored the production of smaller particles (Tabakova *et. al.*, 2007).

Preparation method of copper based catalyst directly affects the catalytic activity of LTWGS reaction. High homogeneity of spinel precursors can be attained by organic acid complex method, urea homogenous coprecipitation, and Pechini method. CO conversion over Cu–Mn oxide catalysts was improved by these methods. In the citric acid complex method, citric or malic acid was utilized for formation of complexes for the preparation of Cu–Mn oxides. An aqueous solution of copper and manganese nitrates was stirred for a definite time and then citric or malic acid was added. The latter procedure was typically followed by the precipitation method. In urea homogenous coprecipitation, an aqueous solution of nitrates and urea was stirred vigorously which is different from the previous method. Pechini method is based on polymerization accompanied with esterification of ethylene glycol (EG) and citric acid (CA). Metals were first placed in the three dimensional polymer matrixes with high homogeneity. Fine oxide particles were then produced by thermal decomposition of the polymer in which the metal complexes were immobilized in the rigid polyester network. The organic acid complex method is a simple way to prepare a catalyst with high activity. High calcination temperature gave rise to high CO conversion over Cu–Mn catalyst derived from the citric acid method as well as NH<sub>3</sub> coprecipitation (Tanaka *et. al.*, 2005).

In the study of Zerva and Philippopoulos (2006), Cu–CeO<sub>2</sub> were prepared by the precipitation method from aqueous and organic solutions (e.g. alcohols) and impregnation was used for active La metal loading. The impregnated ceria support prepared from aqueous solution presented higher activities than those prepared from organic solutions (ethanol, isopropanol, isobutanol, tert-butanol) which was mainly attributed to the fact that organic solutions provided larger crystallites rather than aqueous solutions. Also, the use of organic solvents caused lower specific surface areas and total pore volumes; the low specific surface area had a negative effect on WGS activity of these catalysts. Catalysts

prepared by the coprecipitation method gave the highest activity; however, they had lower specific surface areas than the catalysts prepared by impregnation.

The activity of copper – nickel containing cerium oxide catalysts for LT-WGS was reported by Li *et. al.* (2000). Bulk catalysts were prepared in nanocrystalline form by the urea co-precipitation–gelation method and a lanthanum dopant (10 at.%) was used as a structural stabilizer of ceria, while the Cu or Ni content was in the range of 2–8wt.%. At low metal loadings, Cu or Ni were present in the form of highly dispersed oxide clusters, while at high loadings, clusters as well as particles of CuO or NiO (>10 nm in size) were present on ceria. The WGS activity of Ce(La)O<sub>x</sub> was increased significantly by addition of a small amount (2wt.%) of Cu or Ni. The WGS activity correlates well with an enhanced reducibility of ceria, starting below 200°C for Cu–Ce(La)O<sub>x</sub> and below 300°C for the Ni–Ce(La)O<sub>x</sub> material.

Chen and colleagues (2008) investigated the effects of catalyst type, residence time of reactants in a catalyst bed, reaction temperature and CO/steam ratio on carbon monoxide conversion and hydrogen generation from water gas shift reaction. High temperature catalysts (iron oxide, chromium oxide, chromium trioxide, copper oxide) and low temperature catalysts (copper oxide, zinc oxide, aluminum oxide) were used in the experiments. It was shown that when the residence time is as long as 0.09 s, WGS reaction develops well, no matter which catalyst is used. Increase in reaction temperature promotes the WGS performance by using HTS, while, for the LTS, the reaction is not excited if the reaction temperature is below 200°C. Once the temperature reaches 200°C, reaction occurs but CO conversion decreases with increasing temperature. It was inferred from these results that the WGS reactions with the HTS and the LTS are governed by chemical kinetics and thermodynamic equilibrium, respectively. It was also shown that the H<sub>2</sub> concentration is always higher than that of CO<sub>2</sub> partly due to water decomposition in the WGSR, and in terms of the CO/H<sub>2</sub>O ratio, CO conversion was enhanced when the ratio was decreased to 1/4.

A study on the influence of support (Al<sub>2</sub>O<sub>3</sub>, MgO, SiO<sub>2</sub>-Al<sub>2</sub>O<sub>3</sub>, SiO<sub>2</sub>-MgO, b-zeolite, and CeO<sub>2</sub>) of Cu-ZnO catalysts for the low-temperature water–gas shift reaction was investigated by Yahiro *et. al.* (2007). Supported Cu-ZnO catalysts were prepared by the

conventional impregnation method, followed by the H<sub>2</sub> reduction. The activity of Cu-ZnO catalysts for the WGS reaction was largely influenced by the kind of support; Cu-ZnO catalysts supported on Al<sub>2</sub>O<sub>3</sub>, MgO, and CeO<sub>2</sub> showed high activity, while those on SiO<sub>2</sub>-Al<sub>2</sub>O<sub>3</sub>, SiO<sub>2</sub>-MgO and b-zeolite showed less activity in the temperature range 423–523 K. XRD analysis demonstrated that the copper species were highly dispersed on the supports used in the present study, except for a MgO support. TPR results of a series of supported CuO-ZnO catalysts suggest that the reducibility of CuO is one of the important factors controlling the activity of the WGS reaction over the supported catalysts.

2.3.2.2. Precious Metal Catalysts. Precious metal active components include gold and platinum group metals such as platinum, palladium and ruthenium (Anderson and Boudart, 1982).

Conventional industrial catalysts cannot be used for mobile and small-to-medium-scale fuel cell applications for power generation, mainly due to restrictions in volume, weight, and cost. In addition to high activity, high sustainability against fluctuation from oxidative to reductive atmospheres is essential for the catalysts during the WGS reaction (Shishido *et. al.*, 2009). Generally, the activity of copper-based catalysts is higher for this reaction (Shishido *et.al.*, 2006), but they are less stable to oxidant gases and their catalytic activity decreases as a result of oxidation and/or aggregation of active species. Due to the pyrophoricity, Cu-ZnO-Al<sub>2</sub>O<sub>3</sub> catalysts must be sequestered during system shutdown when only air flows through the system. Furthermore, copper catalysts need to be carefully activated before use, requiring lengthy preconditioning steps. It is evident that novel WGS catalysts need to be developed to meet the necessary criteria for use in fuel processors. Hence, it is vital to develop highly active precious metal catalysts (Shishido *et. al.*, 2009).

Noble metal catalysts may offer significant advantages compared to conventional ones, including high activity in a wider temperature range, no need of activation prior to use, no degradation upon exposure to air or temperature cycles, and availability of conventional wash-coating technologies, which may result in reduced size and weight and improved ruggedness (Panagiotopoulou and Kondarides, 2004).

Ceria-supported precious metals exhibiting high activity comparable to that of conventional Cu/ZnO/Al<sub>2</sub>O<sub>3</sub> catalysts are among the various metal/support combinations investigated for the low-temperature WGS reaction (Panagiotopoulou *et al.*, 2007).

The impact of the Pt promoter loading in Pt/CeO<sub>2</sub> catalysts is very important in the catalyst structural-property relationships. Increasing the Pt loading has a significant impact on catalytic activity. Addition of Pt catalyzes the surface reduction process and reduces the reduction temperature which indicates that higher WGS rates may be attained with higher Pt loading (Jacobs *et al.*, 2005b).

Existence of Pt ions substituted in CeO<sub>2</sub> is the main reason for high CO conversion as well as high reaction rates. In the study by Bera *et al.* (2004), output gas of the ethanol reformer was fed along with the steam to the second reactor (WGS reactor) that contained Ce<sub>1-x</sub>Pt<sub>x</sub>O<sub>2-δ</sub> catalyst prepared by combustion method. In the 125-200°C temperature range 2wt.%Pt-CeO<sub>2</sub> gave higher conversion than 1wt.%Pt-CeO<sub>2</sub>. This higher activity in comparison to low Pt content is attributed to the higher oxygen content. The high oxygen content in 2wt.%Pt-CeO<sub>2</sub> could be due to the decrease in Pt<sup>2+</sup> substitution into Ce<sup>4+</sup> site since amount of Pt particles are higher in 2wt.%Pt-CeO<sub>2</sub> than in 1wt.%Pt-CeO<sub>2</sub>. According to TEM studies over 2wt.%Pt-CeO<sub>2</sub>, a small amount of Pt is present as metal particles and the rest is dispersed as ions that are considered as the active sites in Ce<sub>1-x</sub>Pt<sub>x</sub>O<sub>2-δ</sub> catalysts for LTWGS reaction with high CO conversion, and also, Pt ions substituted in CeO<sub>2</sub> lead to high WGS rates.

Different supports can also be used for the Pt catalysts in LT-WGS reaction. Pt/TiO<sub>2</sub> (R: rutile) catalysts prepared by a conventional impregnation method were evaluated in terms of activity and characteristics by Iida *et al.* (2006). The results indicated that there was a linear relationship between catalytic activity and Pt dispersion and that there was little dependency of catalytic activity on the type of Pt precursors used. The turnover frequency (TOF) for LT-WGS was almost constant regardless of Pt dispersion. According to the results, LT-WGS reaction on Pt/TiO<sub>2</sub> (R) was structure insensitive.

There are several investigations based on enhancing the activity of WGS by adding a second metal to the catalyst. WGS reaction over magnesia-modified Pt/CeO<sub>2</sub> catalysts was

studied by Farias and coworkers (2007). It was shown that the addition of MgO to Pt/CeO<sub>2</sub> increased the activity and stability of the catalyst irrespective of the preparation method, either impregnation or co-precipitation. It was suggested that the addition of magnesium both reduced the carbonate concentration on the catalyst surface during reaction and facilitated ceria reduction favoring the creation of OH groups, which are considered to be the active sites for WGS.

Another study was conducted by Farias and coworkers (2008) for evaluating addition of vanadium oxide into the Pt/CeO<sub>2</sub> catalyst and testing its WGS activity under a feed mixture with composition of 6.0% CO, 16.0% H<sub>2</sub>, 1.6% CO<sub>2</sub>, 0.4% CH<sub>4</sub>, 60.0% H<sub>2</sub>O and N<sub>2</sub> as balance. It was established that over a wider range of temperatures (200-350°C), CO conversion for Pt/6VCeO<sub>2</sub> was higher than unmodified Pt/CeO<sub>2</sub>. Catalyst activity was strongly related to the dispersion of vanadia onto Pt/CeO<sub>2</sub> and increased the catalytic activity up to a vanadium surface density of 6 V atoms/nm<sup>2</sup>, which is below the monolayer coverage. This concentration caused the formation of mono and polyvanadate species. Amongst all V–O bonds established in the molecular structure of vanadium species identified by different spectroscopic techniques, the improvement in WGS reaction kinetics is suggested to be associated with the V–O–Ce bonds; but the generation of tri-dimensional structures with V–O–V bonds led to a gradual drop in activity.

Various metal loadings were investigated by Radhakrishnan and co-workers (2006) in order to compare the activities of metals. A Ce-Zr oxide catalyst was prepared by co-precipitation and then submerged or immersed in Pt, Ru, Rh, Ir, Au, Pd precursor solutions. Noble metal supported ceria-zirconia oxides were tested for their WGS activities in the 200-320°C. The Pt catalyst supported on ceria-zirconia gave the highest activity on a per noble metal basis with a cost and performance optimized loading identified to be in the 1-2wt.% range. The order of WGS activity was Pt > Rh > Ru ≈ Pd > Ir > Au.

Rhenium is considered as another precious metal. The impact on the WGS reaction of using a rhenium promoter for ceria-zirconia supported platinum catalysts was studied by Radhakrishnan *et al.* (2006). Ceria-zirconia (Ce/Zr=58:42) was prepared using urea homogeneous crystallization co-precipitation. Platinum was deposited on calcined oxide using a modified ion-exchange method. The catalyst was suspended in tetrahydrofuran

(THF) and a dissolved rhenium precursor was added to this solution. It was found that rhenium nearly doubled the reaction rate of the supported platinum catalyst in the temperature range of 240-300°C. Rhenium carbonyl was the optimal precursor among perrhenic acid and ammonium per-rhenate precursors. The optimal platinum to rhenium ratio was determined to be about 2:1 by weight with the nominal platinum loading at 2wt.%. Increasing the platinum loading to 3wt.% (without any rhenium addition) provided a similar activity enhancement when compared to the 2:1 Pt/Re sample.

The influence of lanthanum, cerium and samarium over the activity of Ru/Fe<sub>2</sub>O<sub>3</sub> catalysts in the WGS reaction at 300 or 350°C was examined by Basinska and Domka (1999). Much better performance of the catalysts allowing over 90 per cent conversion in WGS reaction was observed by introducing lanthanides, La<sup>3+</sup> and Sm<sup>3+</sup>. The maximum activity of the catalysts was achieved for the molar ratio of Ru:lanthanide = 1:1.

According to the study of Sato and colleagues (2006), among the Ir–Re/TiO<sub>2</sub>, Pt–Re/TiO<sub>2</sub> and Pd–Re/TiO<sub>2</sub> catalysts prepared by incipient wetness method, addition of Re to Ir/TiO<sub>2</sub> catalysts, whose effect is more remarkable than the effect in Pt/TiO<sub>2</sub> and Pd/TiO<sub>2</sub> at the reaction temperature range of 303–473 K. This can be attributed to Re on Ir–Re/TiO<sub>2</sub> catalyst exists as the mixture of partially reduced metal and cationic ReO<sub>x</sub> species, which can be easily oxidized by H<sub>2</sub>O in the reaction atmosphere, as well as easily adsorbing CO (Sato *et al.*, 2006).

In the study of Juan *et al.* (2008), a number of bimetallic gold-ceria catalysts are prepared by co-precipitation technique. These catalysts changing the composition were compared in terms of catalytic activity for LTWGS reaction. Feed compositions used in the experiments are 0.95% CH<sub>4</sub> in 99.05% CO to provide 3 ml/min of this gas mixture together with 40.5 ml/min steam flow (0.03 ml/min liquid water was delivered from a high-performance liquid chromatography pump). Thus, the total weight hourly space velocity (WHSV) was set at about 52,000 h<sup>-1</sup> with the H<sub>2</sub>O/CO ratio of 13.5. They concluded that amongst the entire screened catalysts, 3wt.% (Au–Pt)/CeO<sub>2</sub> displayed the best WGS activity than the monometallic promoters, in the 100–300°C temperature range. They also found that WGS activity was strongly correlated with the surface reducibility which in turn depended on the modified local electronic band structure of promoted ceria.

Gold–ceria catalytic systems over a wide temperature range (140–350°C) and at different space velocities and H<sub>2</sub>O/CO ratios was established by Andreeva and colleagues (2002). Among the catalysts, 3wt.%Au and 5wt.%Au samples manifested comparable activity and stability in the WGS reaction which are higher than those of the 1wt.%Au sample. The Au/CeO<sub>2</sub> sample containing 3wt.% gold exhibits the highest stability. The sample with the lowest gold amount (1wt.%Au/CeO<sub>2</sub>) demonstrates a noticeable decrease in CO conversion when the space velocity was increased. The effect of contact time on the degree of CO conversion for 3wt.%Au/CeO<sub>2</sub> and 5wt.%Au/CeO<sub>2</sub> samples is negligible, especially at higher temperatures. The catalytic activity slightly increases as a function of the H<sub>2</sub>O/CO ratio. Comparing the data obtained for the samples 3wt.%Au/CeO<sub>2</sub> and 5wt.%Au/CeO<sub>2</sub>, it was unexpected that the sample with lower gold loading exhibits even higher CO conversion than the sample with higher gold content.

The WGS activity of dispersed platinum crystallites is directly attributed to the reducibility and oxygen ion mobility of the CeO<sub>2</sub> support. These properties of ceria can be improved by the addition of dopants. The presence of the dopant affects the chemisorptive properties toward CO, and the WGS activity of Pt/Ce catalysts, in a manner which depends on the nature of the dopant cation. In the study of Panagiotopoulou and co-workers (2007), cation (Me)-doped cerium dioxide carriers (Me = Ca, La, Mg, Zn, Zr, Yb, Y, Gd) were prepared by the urea-nitrates combustion method that the dopant cations are incorporated into the ceria lattice. It is observed that the specific reaction rate per gram of catalyst at 250 °C depends strongly on the nature of the promoter used, following the order of Yb>Gd>Zr>Mg>La>CeO<sub>2</sub>(undoped)>Ca>Y>Zn, with the rate for the Yb-promoted catalyst being about one order of magnitude higher than that for the Zn-promoted sample (Panagiotopoulou *et al.*, 2007).

The promotion of Pt/ceria catalysts with alkali metals over LTWGS reaction is an optimization issue. The lower alkali dopant leads to increment of the catalytic activity, but on the other hand high levels of dopants cause lower conversion. This lower activity may be attributed to the covering of the Pt surface by the alkali and hindering the synergism involved between Pt and ceria in the catalytic mechanism. In the study of Evin and co-workers (2008), the catalytic activity tests were performed at the temperatures of 200–300°C, and 2wt.%Pt-CeO<sub>2</sub> catalyst was used as the reference case for comparison with

high alkali doped (2.5%Na, 4.3%K, 9.3%Cs, 14.5%Rb) and low alkali doped catalysts (0.5%Na, 0.9%K). Increasing the amount of alkali to too high a level leads to other negative factors, including decreased BET surface area, blocking of the Pt surface sites, and a shift in the temperature of the surface shell reduction step of ceria. As a result, if the alkalinity is too high, the CO conversion rate during water–gas shift decreases. At lower levels of alkali, however, it was demonstrated that the negative factors previously mentioned can be avoided such that one may take advantage of the weakening of the formate C–H bond and improve the overall turnover frequency during water–gas shift. This was demonstrated at 0.5%Na and 0.9%K doping levels.

The reduction time is another parameter that can affect the activity of the reaction, which also may cause the catalyst deactivation. Irreversible over reduction of the catalyst with 1.5wt.% platinum loading determined by inductively coupled plasma analysis over ceria–zirconia based support leads to rapid deactivation of Pt/ceria water-gas shift catalyst systems operating under feed conditions typical of a reformer outlet. Deactivation rates observed translate into catalyst half-lives that are too short to be practical in an automotive application. Significantly lower deactivation rates were observed when hydrogen was not present in the feed. Attempts to rejuvenate the catalyst by heating under steam and under air were unsuccessful. (Zalc *et al.*, 2002).

Catalyst stability with time on stream is one key factor that must be taken into account when considering commercial applications of the catalyst. The relationships between the catalyst stability and the addition of Re to Pt/TiO<sub>2</sub> was investigated in the study of Azzam *et al.* (2007). The catalyst showed almost no deactivation during 20 h time on stream. It is remarkable that Re not only stabilized the Pt/TiO<sub>2</sub> catalyst, but also enhanced activity and the rate of H<sub>2</sub> production. Re addition was also investigated by Iida and Igarashi (2006). The findings indicated that Re addition to Pt catalysts resulted in a decrease in the strength of CO adsorbed on the Pt/TiO<sub>2</sub> (rutile). It was therefore thought that the decreasing strength of CO brought about an increase in the reactivity of the adsorbed CO species due to Re addition.

In addition to the use of more than one metal additive on catalyst, the nature of the support is another critical issue evaluated in terms of WGS activity. Panagiotopoulou and

Kondarides (2006) stated that the WGS activity of supported noble metal catalysts depends strongly on the nature and physicochemical characteristics of the support. In particular, it was found that activity of noble metals is significantly improved when supported on “reducible” ( $\text{TiO}_2$ ,  $\text{CeO}_2$ ,  $\text{La}_2\text{O}_3$ , and YSZ) rather than on “irreducible” ( $\text{Al}_2\text{O}_3$ ,  $\text{MgO}$ , and  $\text{SiO}_2$ ) metal oxides. According to this study, platinum catalysts are generally more active than Ru, Rh, and Pd so that the activity follows the order of  $\text{Pt} > \text{Rh} \approx \text{Ru} > \text{Pd}$ , with Pt being 15–20 times more active than Rh and Ru and 50 times more active than Pd, at  $250^\circ\text{C}$  using a feed stream consisting of 3% CO and 10%  $\text{H}_2\text{O}$  (balance He). Platinum catalysts supported on  $\text{CeO}_2$ ,  $\text{La}_2\text{O}_3$ , and YSZ are active at temperatures higher than  $200^\circ\text{C}$  and reach equilibrium conversions at ca  $450^\circ\text{C}$ , while  $\text{Al}_2\text{O}_3$ -supported samples become active at sufficiently higher temperatures.

In the study of Kim *et al.* (2009), the effect of support in terms of reducibility and irreducibility over the WGS activity was presented based on the amount of chemisorbed CO among supported Pt-Ce catalysts. The normalized reaction rate of Pt-Ce catalysts supported on reducible metal oxides such as Pt-Ce/ $\text{TiO}_2$ , Pt-Ce/ $\text{ZrO}_2$ , Pt-Ce/YSZ and Pt-Ce/ $\text{CeO}_2$  is almost same. On the other hand, the normalized reaction rate among Pt-Ce catalysts supported on irreducible metal oxides decreased in the following order: Pt-Ce/ $\text{SiO}_2$  > Pt-Ce/ $\gamma$ - $\text{Al}_2\text{O}_3$  >> Pt-Ce/ $\text{SiO}_2$ - $\text{Al}_2\text{O}_3$ . Based on the normalized reaction rates, the reducible metal oxides can be considered to be better as a support than the irreducible metal oxides in a parallel with Panagiotopoulou and Kondarides (2006). Pt-Ce/ $\text{TiO}_2$  showed the highest turnover frequency among tested catalysts (Kim *et al.*, 2009).

1 wt.%Pt- $\text{CeO}_2$ , 1 wt.%Au- $\text{CeO}_2$ , 3 wt.%Au- $\text{Fe}_2\text{O}_3$  catalysts were synthesized by using the sol-gel, co-precipitation, both co-precipitation and deposition-precipitation methods respectively. Interestingly, when comparing the effect of preparation method on Au- $\text{Fe}_2\text{O}_3$  catalyst, it was found that deposition-precipitation gave higher CO conversion than co-precipitation. The catalysts were tested for their activities in a gas mixture typically containing 4% CO, 2.6%  $\text{H}_2\text{O}$  and helium. The lowest activity is shown by highly crystalline ceria containing Au- $\text{CeO}_2$  catalyst. Water vapor content significantly enhanced the catalytic performance of Pt- $\text{CeO}_2$  catalyst in the temperature range of  $200$ – $360^\circ\text{C}$ . On the other hand, the water content has slightly less of an effect on the activity of Au- $\text{CeO}_2$  and moderately influenced Au- $\text{Fe}_2\text{O}_3$  catalysts in the reaction temperature range of  $300$ –

360°C. CO conversion increases with an increase in the reaction temperature over Pt-CeO<sub>2</sub> sol-gel catalyst. However, CO conversion decreases with increasing CO concentration in the feed. The decrease with increasing CO concentration is most likely due to the well-known poisoning effect of CO on Pt sites. Similar effect was also observed on Au-CeO<sub>2</sub> and Au-Fe<sub>2</sub>O<sub>3</sub> catalysts (Luengnaruemitchai *et al.*, 2003).

The effects of various portions of metal loadings on monolithic catalyst were studied. They found that the optimum loading was 50wt.% for Ce<sub>0.8</sub>Zr<sub>0.2</sub>O<sub>2</sub> loading, 0.68wt.% for Pt loading and 3 for Pt/Re weight ratio. Re addition can reduce half of the Pt loading required to reduce CO outlet content to around 1%. According to their pyrophoricity tests, no obvious activity loss was observed over 0.11wt.%Re/0.34wt.%Pt/50wt.%Ce<sub>0.8</sub>Zr<sub>0.2</sub>O<sub>2</sub>-M/cordierite (optimized composition) catalyst after three exposures to oxygen (Du *et al.*, 2008).

## 2.4. Water Gas Shift Catalysts

### 2.4.1. Particulate Catalysts

2.4.4.1. Platinum as a catalyst. Recent developments of fuel cell technology also need active precious metal catalysts for reforming, shift reaction, preferential oxidation, and electrode reaction (Ayabe *et al.*, 2003). These precious metal catalysts are generally prepared by depositing fine particles of metal on a porous oxide or carbon support by the impregnation technique from an aqueous suspension (Okanishi *et al.*, 2006).

In general, it is generally accepted that the reaction over supported noble catalysts occurs in a bifunctional manner, such as adsorption/activation of CO and adsorption/activation of H<sub>2</sub>O. Former is implemented by dispersed metallic phase, while the latter is implemented by metal oxide support (Panagiotopoulou *et al.*, 2007).

When platinum is dispersed on composite MO<sub>x</sub>/Al<sub>2</sub>O<sub>3</sub> carriers, a fraction of Pt crystallites is expected to be in direct contact with reducible MO<sub>x</sub> species. It may then be suggested that this fraction should be responsible for the higher activity of Pt/MO<sub>x</sub>/Al<sub>2</sub>O<sub>3</sub> catalysts at low temperatures, compared to Pt/Al<sub>2</sub>O<sub>3</sub> (Panagiotopoulou *et al.*, 2007).

2.4.4.2. Ceria as a catalyst. Ceria oxide is classified as an n-type semiconducting oxide with extremely high oxygen mobility where its electronic conductivity and oxygen vacancy can be easily altered by using different promoters and different testing conditions. A number of unique properties associated with ceria have been recognized including high redox properties, maintaining high dispersion for metal nano-particles, hence giving high activity for CO oxidation at low temperature and high WGS activity (Juan *et al.*, 2008).

The role of CeO<sub>2</sub> is associated with high oxygen-storage capacity. CeO<sub>2</sub> is also serving as a stabilizer of both the noble metal and alumina, as well as a promoter of several reactions including the water-gas shift and carbon monoxide oxidation (Li *et al.*, 2000). Addition of MO<sub>x</sub> may also affect the chemisorptive properties of the supported noble metal by altering chemisorption strength and/or by creating new active sites (Panagiotopoulou *et al.*, 2007).

Cerium oxide-containing WGS catalysts are promising because of the oxygen storage capacity of ceria and the cooperative effect of ceria-metal leading to highly active sites. It is not used alone as catalyst, but it is usually employed in combination with other oxides or in conjunction with active metals and thermally stable supports. The CeO<sub>2</sub> is of comparatively little interest as catalyst because of its textural stability, which is not high enough to meet the requirements of high-temperature gas-phase catalytic reactions. Another factor, which discourages the use of pure ceria, is its cost, which is higher than that of more common supports. Ceria is a crucial component of automotive, three way, emissions control catalysts partly because it promotes precious-metal catalysts for the WGS reaction (Trovarelli *et al.*, 2001).

A number of functions have been ascribed to ceria, including promoting WGS activity (Diwell *et al.*, 1991), maintaining the dispersion of the catalytic metals (Gandhia and Shelefa, 1987) and stabilizing the surface area of the support (Ozawa and Kimura, 1990). In addition, it also promotes precious metal catalysts for WGS reaction (Whittington *et al.*, 1995).

2.4.4.3. Alumina as a support. The support materials, such as alumina, silica, and active carbon, possess large surfaces to provide sufficient area for depositing fine grains of a

precious metal. These inert supports generally do not interact chemically with the supported metal. However, a series of oxide supports often exhibit strong chemical interaction with metallic components (Roth *et al.*, 2001). This phenomenon is sometimes explained as strong metal–support interaction (SMSI) (Okanishi *et al.*, 2006).

#### **2.4.2. Monolithic Catalysts**

Monolithic supports are structures that composed of interconnected repeating cells or channels. They are most commonly composed of ceramic or metal materials but some can also be made of plastic. The most important physical characteristics when used as a catalyst support is the size of the channel through which the gaseous reactants and products traverse (Hecka *et al.*, 2001).

The number of channels, their diameters and wall thickness determine the cell density, expressed as cells per square inch (cpsi), which in turn allows the calculation of the geometric surface area, the sum of the areas of all the channel walls upon which the catalyst is deposited. This leads to one of the most important advantages of the monolith in that it has a large open frontal area resulting in very little resistance to flow and hence low pressure drop. The lower the pressure drop the lower the resistance to flow or back pressure on the system and hence lower the energy loss (Hecka *et al.*, 2001).

The active catalyst is deposited as a washcoat onto the geometric surface of the monolithic structure. The washcoat is a mixture of active catalyst components, stabilizers, and a high surface area coating layer based on alumina (Giroux *et al.*, 2005).

### 3. EXPERIMENTAL WORK

#### 3.1. Materials

##### 3.1.1. Chemicals

All the chemicals used in catalyst preparation are listed in Table 3.1. Tetraammineplatinum (II) nitrate, cerium (III) nitrate hexahydrate and aluminum oxide were used in the preparation of particulate catalysts while the aluminum oxide colloidal dispersion was used in the preparation of monolithic catalysts.

Table 3.1. Chemicals used in catalyst preparation

Chemicals	Formula	Grade	Source	Molecular Weight (g.mol <sup>-1</sup> )
Tetraammineplatinum (II) nitrate	Pt(NH <sub>3</sub> ) <sub>4</sub> (NO <sub>3</sub> ) <sub>2</sub>	Research	Aldrich	387.21
Cerium (III) nitrate hexahydrate	Ce(NO <sub>3</sub> ) <sub>3</sub> .6H <sub>2</sub> O	Extra pure	Merck	434.23
Aluminum Oxide	$\gamma$ -Al <sub>2</sub> O <sub>3</sub>	Extra pure	Zeochem EU	101.96
Aluminum Oxide Colloidal Dispersion	Al <sub>2</sub> O <sub>3</sub>	Research	Alpha Aesar	101.96

##### 3.1.2. Gases and Liquids

The gases used in this study H<sub>2</sub>, Ar and CO were supplied by Birleşik Oksijen Sanayi (BOS) and CO<sub>2</sub> is obtained from Linde Company, Istanbul, Turkey. The applications and specifications of the liquids and gases used in this study are listed in the Tables 3.2 and 3.3.

Table 3.2. Applications and specifications of the liquids used

Liquid	Application	Specification
Water	Reactant, Aqueous solutions	Distilled

Table 3.3. Applications and specifications of the gases used

Gas	Application	Specification
Carbon monoxide	Reactant, GC calibration	99.5%
Carbon dioxide	Reactant, GC calibration	99.995%
Nitrogen	Reactant (inert), GC calibration	99.998%
Hydrogen	Reducing agent, GC calibration	99.99%
Argon	GC carrier	99.999%

### 3.2. Experimental System

The experimental system used in current study consists of mainly three groups:

- Catalyst Preparation System: These systems are for applications of the sequential impregnation method for loading metals on particulate catalysts and of the co-impregnation method for the coating of monoliths with alumina and metal loading.
- Micro-reactor flow system: This system consists of automated reactant flow system and a temperature controlled reactor and is used for reaction tests.
- Product analysis system: In this system, the compositions of the reactant and product gases are analyzed by using a gas chromatograph.

#### 3.2.1. Catalyst Preparation System

Particulate catalysts were prepared by the sequential impregnation method whereas monolithic catalysts were prepared by both wash coating and co-impregnation method.

1.4wt.%Pt-5wt.%CeO<sub>x</sub>/γ-Al<sub>2</sub>O<sub>3</sub> and 1.4wt.%Pt-10wt.%CeO<sub>x</sub>/γ-Al<sub>2</sub>O<sub>3</sub> particulate catalysts were prepared by sequential impregnation method using the experimental system in Figure 3.1.

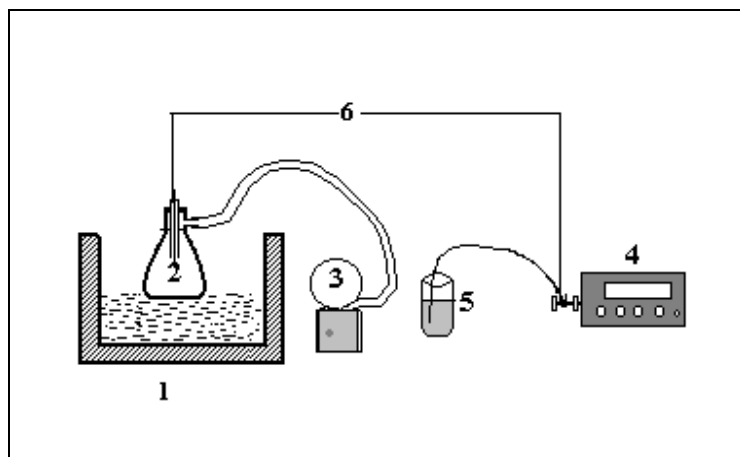


Figure 3.1. The impregnation system of particulate catalysts: 1. Ultrasonic mixer 2. Vacuum flask 3. Vacuum pump 4. Peristaltic pump 5. Beaker 6. Silicone tubing (Akin, 1996)

1.4wt.%Pt-5wt.%CeO<sub>x</sub>/γ-Al<sub>2</sub>O<sub>3</sub> cordierite monoliths were wash-coated with alumina by using the system in Figure 3.2. Alumina wash-coated monoliths were impregnated with Pt and Ce precursors by using the system presented in Figure 3.3.

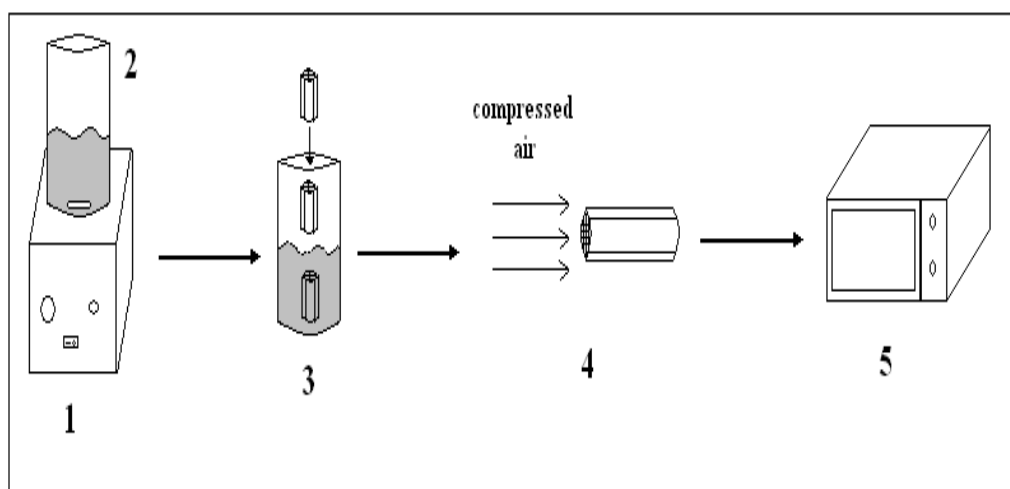


Figure 3.2. The alumina wash-coating system: 1. Magnetic Mixer 2. Beaker 3. Dipping Procedure 4. Compressed Air Flow 5. Microwave Oven (Döker, 2008)

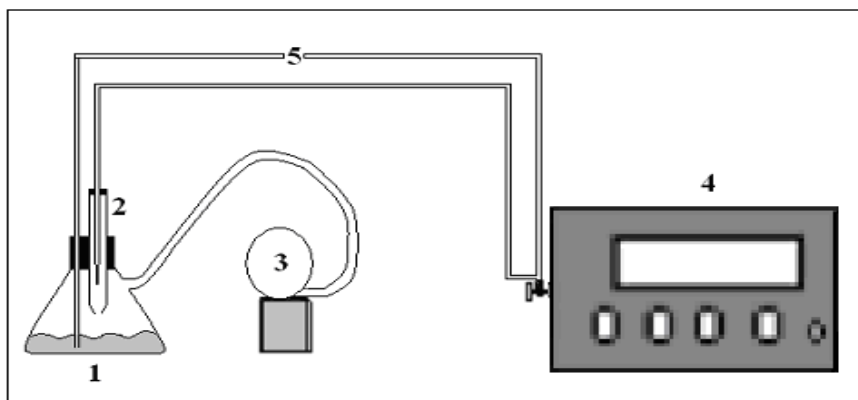


Figure 3.3. The impregnation system of monolithic catalysts: 1. Vacuum Flask 2. Glass tube 3. Vacuum pump 4. Peristaltic pump 5. Silicone tubing (Döker, 2008)

### 3.2.2. Reaction Section

The reaction section consisted of a 2.6 cm ID x 46.5 cm tube furnace and stainless steel fixed-bed down-flow micro-reactors of two different diameters, 4 mm ID x 59.8 cm for particulate catalysts, and 11.5 mm ID x 59.8 cm for monolithic catalysts.

The reactors were longer than the furnace to assemble stainless steel fittings easily during catalyst charging and recharging. The micro-reactor was installed in the furnace controlled by a Shimaden FP-21 programmable temperature controller with  $\pm 0.5$  K sensitivity. The catalyst bed was kept in fixed position by plugging the lower end with silane treated glass wool. The catalyst bed was placed in the center of the reactor which was in the constant-temperature region of the furnace. The temperature of catalyst bed was measured by 20-gauge wire K-type sheathed thermocouple installed near the center of the catalyst bed just outside the micro-reactor wall. The reactor and furnace system is presented in Figures 3.4 and 3.5. It is important to prevent heat loss and maintain stable temperature profile, so this was accomplished by placement of ceramic wool at both inlet and outlet of the reactor-furnace. The function of closing on-off valve at the end of the reactor was to prevent back flow of the feed mixture into the reactor during feed analysis.

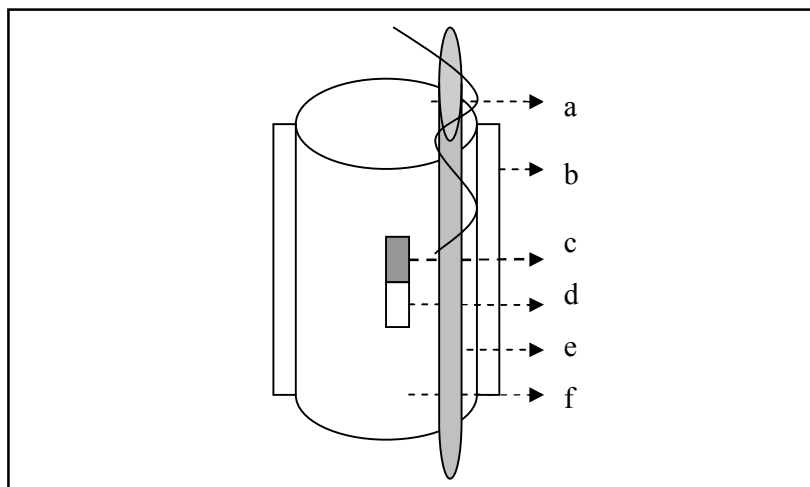


Figure 3.4. Schematic diagram of the reactor and furnace system: a. Thermocouple  
b. Ceramic wool insulation c. Catalyst d. Catalyst bed e. Furnace f. Reactor

### 3.2.3. Product Analysis Section

CO, H<sub>2</sub>, N<sub>2</sub> gas streams were analyzed using an HP-Agilent 6890N Network temperature-programmable gas chromatograph with a thermal conductivity detector (TCD). The details of the analysis system are given in Table 3.4.

Table 3.4. Reactant and product gas analysis conditions

Column Type	Packed Column
Detector Type	Thermal Conductivity
Column Oven Temperature	40°C
Injector Temperature	40°C
TCD Temperature	150°C
Carrier Gas	Argon
Carrier Gas Flow Rate	40 ml.min <sup>-1</sup>
Column Packing Material	Molecular Sieve 5A, 60-80 mesh
Column Tubing Material	Stainless Steel
Column ID & Length	1/8" OD x 2 m
Sample Loop	1 ml

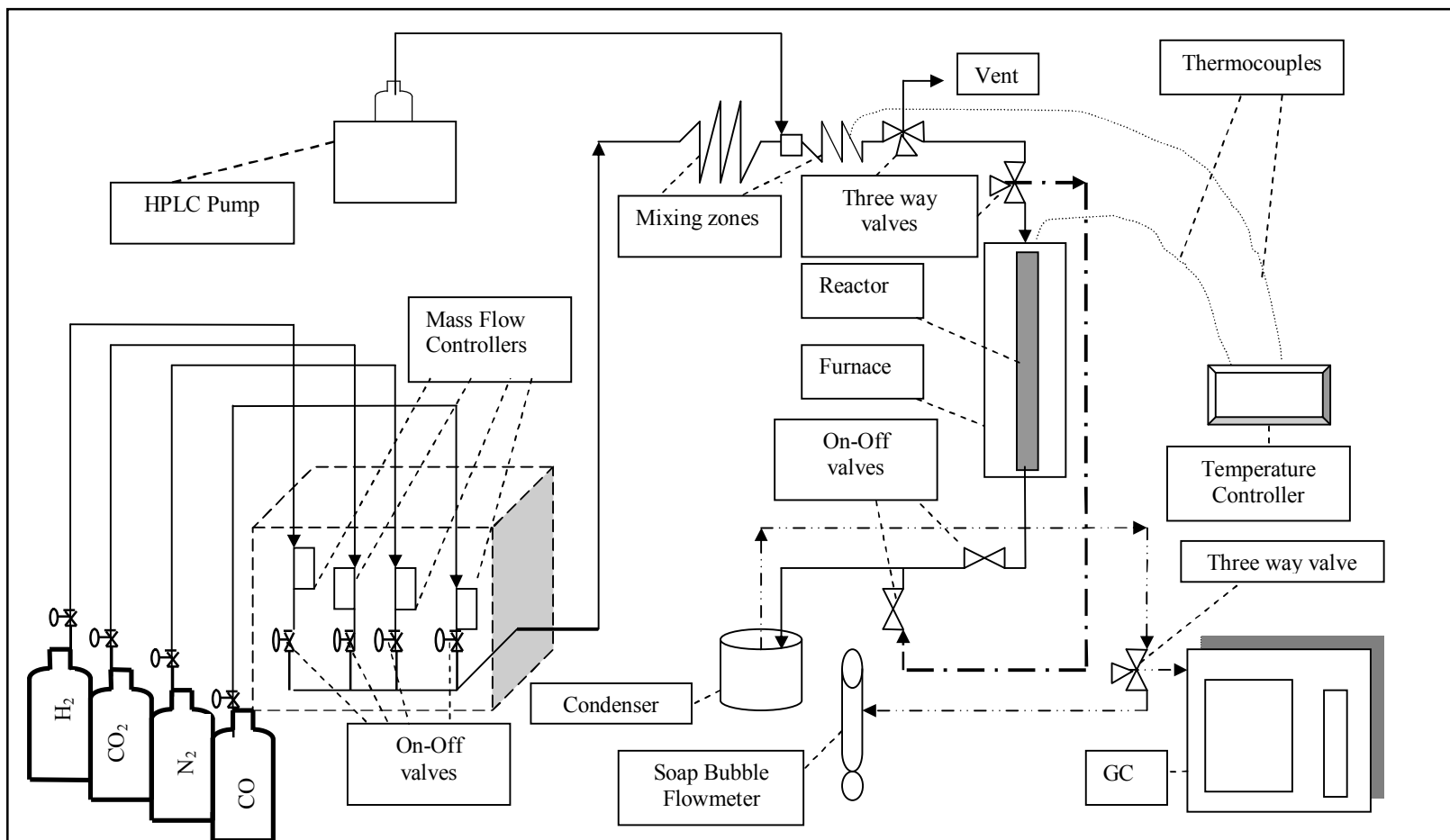


Figure 3.5. The micro-reactor flow and product analysis system (Şen, 2008)

### 3.3. Catalyst Preparation

#### 3.3.1. Incipient Wetness Impregnation Procedure

The Pt-CeO<sub>x</sub>/γ-Al<sub>2</sub>O<sub>3</sub> catalyst used in the majority of the experiments was prepared according to a composition of 1.4wt.%Pt-5wt.%CeO<sub>x</sub>/γ-Al<sub>2</sub>O<sub>3</sub>, taking into consideration the results reported by Şen (2008).

Particulate catalyst was prepared by the sequential impregnation method using the system in Figure 3.1. The impregnation procedure consisted of four steps:

- Evacuating the support
- Contacting the support with the precursor solution
- Drying
- Calcination

The particle size of the support is so important that it is directly related to whether the metals is loaded efficiently or not, which in turn affects the catalytic activity. Commercial γ-alumina support was crushed and sieved into 45-60 mesh size (344-255 μm). It was dried in a vacuum oven at 105°C for 1 hour and then calcined in a muffle furnace at 450°C for 5 hours. 5 g of alumina support was put in a vacuum flask and was kept under vacuum in the first step of the preparation of catalysts by incipient wetness impregnation method. The vacuum pump was also kept on during the addition of the precursor solution since the trapped air in the pores of the support could prevent complete penetration of the solution. Thus, more uniform distribution of the active component is obtained by removing the trapped air. The support material in the vacuum flask was mixed under vacuum with an ultrasonic mixer for 30 minutes before impregnation.

The calculated amount of cerium nitrate salt was dissolved in 1.21 cm<sup>3</sup> of distilled water per gram of alumina support. Aqueous cerium nitrate solution was fed to the vacuum flask at a flow rate of 0.5 ml.min<sup>-1</sup> via silicone tubing using a Masterflex computerized-drive peristaltic pump. The slurry was mixed ultrasonically during impregnation to maintain uniform distribution of the cerium nitrate solution. After all the cerium nitrate

solution was fed, the mixing was continued for an additional 90 minutes. The resulting slurry was dried at 115°C overnight (16 hours) and then was calcined at 400°C in a muffle furnace for 2 hours to obtain CeO<sub>x</sub>/γ-Al<sub>2</sub>O<sub>3</sub>.

The calculated amount of Pt precursor salt was dissolved in distilled water and the aqueous solution of Pt was added to the dried, calcined and ceria impregnated alumina catalyst with the same procedure described above. After impregnation, the resulting slurry of Pt-CeO<sub>x</sub>/γ-Al<sub>2</sub>O<sub>3</sub> catalyst was dried at 115°C overnight (16 hours) and calcined at 400°C for 2 hours to obtain Pt-CeO<sub>x</sub>/γ-Al<sub>2</sub>O<sub>3</sub>.

### **3.3.2. Wash-coating and Co-impregnation Procedure**

3.3.2.1. Wash-coating with colloidal alumina solution. Monolithic catalysts entail wash-coating of alumina since the monolith structure is composed of cordierite, a kind of ceramic. This is the main distinction between the preparation procedures of particulate and monolithic catalysts. To form a wash-coat layer on a monolithic substrate is accomplished by using a colloidal solution of the wash-coat material (Nijhuis *et. al.*, 2001). Colloidal solutions of alumina are commercially available, and a 20 weight per cent colloidal alumina solution from Alpha Aesar was used in this study for applying this method.

The wash-coating procedure was developed with three 400 cpsi cordierite monoliths cut in cylinders of 11 mm diameter and 10 mm length before coating (Döker, 2008). The pretreated monoliths were weighed and then dipped vertically into the colloidal alumina solution for two minutes. Excess suspension was evacuated from the channels by a flow of compressed air. In order to fix the colloidal alumina, monoliths were dried in a microwave oven for 45 minutes at 180W. Alumina coated monoliths were kept in a desiccator for 15 minutes, since they are hot, they can absorb moisture easily if one measures the weight increment immediately after microwave drying. Then, the monoliths were weighed. The procedure was repeated until a 13-15 weight per cent increase was obtained. The wash-coated monoliths were calcined in air at 973 K for two hours, with a temperature ramp of 2.5 °C min<sup>-1</sup>.

3.3.2.2. Co-impregnation method. Figure 3.2. was used for preparation of 1.4wt%Pt-5wt.%CeO<sub>x</sub> supported on alumina wash-coated monoliths. The co-impregnation procedure comprised three steps:

- Contacting the wash-coated monolith with the precursor solution
- Evacuating the channels by compressed air
- Microwave drying
- Calcination

For wet impregnation, the precursor solution containing both Pt and Ce salts was firstly put into the vacuum flask and one end of the silicone tubing was dipped into the precursor solution. The other end of the silicone tubing was used to feed the precursor solution to the open-ended glass tube. One alumina wash-coated cordierite monolith was placed in the open-ended glass tube that was fixed into a vacuum flask by a plastic cork, and then the vacuum pump and peristaltic pump were operated simultaneously. The vacuum pump was used to remove the excess liquid in the channels of the monolith and to give a uniform distribution of the active components. After the first droplet of the precursor solution dripped, the monoliths were impregnated for 15 minutes, and the impregnated monolith was dried in a microwave oven operated at 180W for 40 minutes and then calcined overnight (16 hours) at 550°C.

#### **3.4. Catalytic Activity Measurements**

125 mg of both particulate and monolithic catalysts was used during experiments for testing the catalytic activity and stability with pure feed containing carbon monoxide and steam and with mixed feed containing CO<sub>2</sub> and/or H<sub>2</sub> product. The concentrations of inlet gases were adjusted by balancing the diluent inert gas, N<sub>2</sub>. All experiments were carried out at a total gas flow rate of 100 ml/min.

The activity tests were carried out in the microreactor flow system depicted in Figure 3.5. All the catalysts were reduced with H<sub>2</sub> before the reaction. Heating from 25°C to the reduction temperature followed by cooling to the reaction temperature after reduction were performed under the N<sub>2</sub> flow. The outline of the reduction program for Pt-CeO<sub>x</sub>/γ-Al<sub>2</sub>O<sub>3</sub>

catalyst and reaction conditions for catalytic activity tests are given in Table 3.4. and Table 3.5, respectively.

Table 3.5. Reduction program for Pt-CeO<sub>x</sub>/γ-Al<sub>2</sub>O<sub>3</sub> catalysts

Segments	Starting and End Temperatures	Segment Gas
First Segment	Heating from 25°C to 350°C with a heating rate 5°C.min <sup>-1</sup>	N <sub>2</sub> with flow rate of 50 ml.min <sup>-1</sup>
Second Segment (Reduction)	Keeping constant at 350°C for 3h	H <sub>2</sub> with flow rate of 50 ml.min <sup>-1</sup>
Third Segment	Flushing at 350°C for 1h to clean the catalyst surface	N <sub>2</sub> with flow rate of 50 ml.min <sup>-1</sup>
Fourth Segment	Cooling down to reaction temperature	N <sub>2</sub> with flow rate of 25 ml.min <sup>-1</sup>

Table 3.6. Reaction conditions for catalytic activity tests

Parameter	Value
γ-Al <sub>2</sub> O <sub>3</sub> Support Particle Size (μm)	45-60 mesh size (344-255)
Catalyst Amount (mg)	125
Reaction Temperature (°C)	225-300
Reaction Total Flow Rate (ml/min)	100
W/F Ratio (mg.min.ml <sup>-1</sup> )	1.25

## 4. RESULTS AND DISCUSSION

The objective of this study was to investigate the low-temperature water-gas shift performance of Pt-ceria catalysts supported on particulate and monolithic structures using both pure and mixed realistic feed compositions in the 225-300°C range. The particulate catalysts studied were divided into two groups according to their cerium oxide loading, 1.4wt.%Pt-5wt.%CeO<sub>x</sub>/γ-Al<sub>2</sub>O<sub>3</sub> and 1.4wt.%Pt-10wt.%CeO<sub>x</sub>/γ-Al<sub>2</sub>O<sub>3</sub> which were prepared by the sequential impregnation method whereas co-impregnation was used for preparing alumina wash-coated monoliths with 1.4wt.%Pt-5wt.%CeO<sub>x</sub> composition. Catalytic activity tests were conducted in a micro-reactor flow system at atmospheric pressure at 225, 250, 275 and 300°C. The effects of the H<sub>2</sub>O/CO ratio, H<sub>2</sub> or CO<sub>2</sub> addition to the feed, and the co-existence of H<sub>2</sub> and CO<sub>2</sub> in the feed were studied with a view to compare particulate and monolithic catalysts of similar composition.

Since water gas shift (WGS) is a mildly exothermic equilibrium-limited reaction, equilibrium CO conversion decreases with increasing temperature, which constitutes the main reason for using LTWGS converters in fuel processors. However, from the kinetics standpoint, the challenge is to design catalysts that are active enough to reach equilibrium at low temperatures. Some LTWGS catalysts are deactivated by water at low temperatures, the optimum temperature bracket for base metal oxides is 200-250°C where CO conversion still decreases when the temperature decreases from the high limit to the low limit (Tanaka *et al.*, 2003a). Moreover, in a fuel processor, the reformer effluent is directly introduced to the WGS reactor as a feed stream which suppresses CO conversion to low values according to Le Chatelier's Principle, because of the existence of H<sub>2</sub> and CO<sub>2</sub>. Thus, it is important to find the best H<sub>2</sub>O/CO ratio that promotes the LTWGS reaction in the forward direction for the product side.

Approximately the lower limit temperature of LTWGS, 225°C, was chosen to see up to what extent the CO conversion over 1.4wt.%Pt-5wt.%CeO<sub>x</sub>/γ-Al<sub>2</sub>O<sub>3</sub> is enhanced by increasing the H<sub>2</sub>O/CO ratio in the pure feed. This ratio is also utilized to drive the WGS reaction to the product side in case of H<sub>2</sub> and CO<sub>2</sub> existence in feed mixture for

overcoming the product effect. After choosing the best ratio, parametric studies were conducted by the addition of both H<sub>2</sub> and CO<sub>2</sub> to the feed stream at different temperatures.

Parametric studies involving the addition of only H<sub>2</sub>, only CO<sub>2</sub>, both H<sub>2</sub> and CO<sub>2</sub> were also carried out for the H<sub>2</sub>O/CO ratio of 3/1 studied by Şen (2008) using pure feed streams. Addition of both H<sub>2</sub> and CO<sub>2</sub> to the feed stream was also performed at the 250 and 275°C to cover the temperature range of LTWGS reaction. Realistic feed mixture containing H<sub>2</sub> and CO<sub>2</sub> was also utilized for testing the 1.4wt.%Pt-10wt.%CeO<sub>x</sub>/γ-Al<sub>2</sub>O<sub>3</sub> catalyst in which the amount of CeO<sub>x</sub> impregnated on the particulate catalyst is doubled to assess the effect of CeO<sub>x</sub> content on CO conversion. The catalytic activity properties of monolithic catalysts having similar Pt metal and CeO<sub>x</sub> promoter loadings as the 1.4wt.%Pt-5wt.%CeO<sub>x</sub>/γ-Al<sub>2</sub>O<sub>3</sub> particulate catalyst were also tested using the realistic mixed feed composition.

The WGS activity of each catalyst was expressed in terms of the percentage of CO converted using the Equation 4.1:

$$\text{CO conversion (\%)} = \frac{[\text{CO}]_{in} - [\text{CO}]_{out}}{[\text{CO}]_{in}} \times 100 \quad (4.1)$$

[CO]<sub>in</sub> and [CO]<sub>out</sub> are the carbon monoxide concentrations in the reactor feed and effluent, respectively.

The amount of liquid water used in the experiments was calculated by Equation 4.2:

$$V_{\text{Steam}(H_2O)} = \frac{V_{\text{Liquid}(H_2O)} \times \rho_{H_2O} \times R \times T}{M_{H_2O} \times P} \quad (4.2)$$

Where  $\rho=1000\text{g.L}^{-1}$ ;  $P=1\text{ atm}$ ;  $R=0.082\text{ L.atm.mol}^{-1}.\text{K}^{-1}$ ;  $T=298\text{ K}$  and  $M_{H_2O}=18\text{ g.mol}^{-1}$ .

All experiments were carried out with 100 cm<sup>3</sup>/min total flow; the composition of the reactor outlet stream was measured at 30-minute intervals for 3 hours.

#### 4.1. Effect of H<sub>2</sub>O/CO Ratio

The LTWGS activity of the 1.4wt.%Pt/5wt.%CeO<sub>x</sub>/γ-Al<sub>2</sub>O<sub>3</sub> particulate catalyst was studied at 225°C and five different H<sub>2</sub>O/CO ratios of 1, 2, 3, 5 and 7; the results are presented in Table 4.1 and Figure 4.1. The CO concentration in the feed was kept constant at 5 mol% and the H<sub>2</sub>O/CO ratio was adjusted by changing the H<sub>2</sub>O concentration, keeping the total gas flow rate constant at 100 cm<sup>3</sup>/min by altering the percentage of inert N<sub>2</sub>.

The catalyst activity increased significantly with increasing H<sub>2</sub>O/CO from 1 to 2, while further increase in the H<sub>2</sub>O/CO ratio from 2 to 3 produced a smaller improvement. Experiments with further H<sub>2</sub>O/CO ratio increases were performed with 5 and 7. It is interesting to note that, with each increase in the H<sub>2</sub>O/CO ratio to the next higher value, the increase observed in CO conversion is higher than in the previous increase. For instance, increasing the pure feed H<sub>2</sub>O/CO ratio from 3 to 5 causes an incremental increase of 5% in CO conversion; when the feed H<sub>2</sub>O/CO ratio is raised from 5 to 7, incremental increase in CO conversion is 7%, which is higher than the previous incremental increase of 5%.

Table 4.1. Effect of H<sub>2</sub>O/CO ratio on CO conversion at 225°C over 1.4wt.%Pt-5wt.%CeO<sub>x</sub>/γ-Al<sub>2</sub>O<sub>3</sub>

Time(min)	H <sub>2</sub> O/CO				
	1	2	3	5	7
	CO conversion (%)				
30	7.32	13.26	15.81	20.81	31.42
60	10.01	13.82	15.94	20.47	26.56
90	10.07	14.19	15.78	19.19	26.38
120	10.52	13.62	14.90	20.47	26.89
150	10.36	13.82	15.11	20.20	26.94
180	7.50	12.10	13.99	19.15	26.91

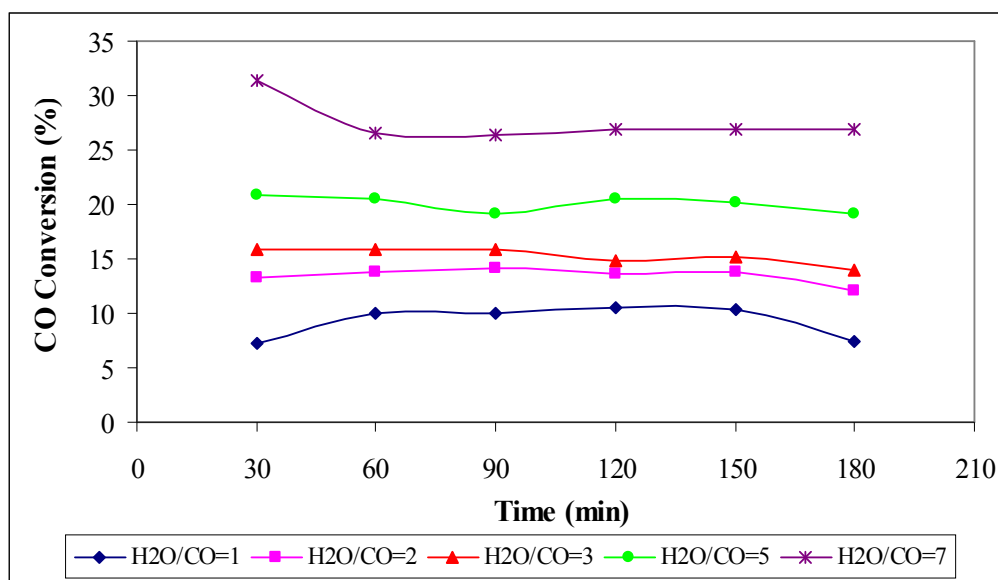


Figure 4.1. Effect of H<sub>2</sub>O/CO ratio on CO conversion at 225°C over 1.4wt.%Pt-5wt.%CeO<sub>x</sub>/γ-Al<sub>2</sub>O<sub>3</sub>

In a product-free feed gas mixture containing 2 mol% CO and 10.7 mol% H<sub>2</sub>O in helium by using a 0.8wt.%Pt/CeO<sub>x</sub> catalyst prepared by deposition precipitation, around 40% CO conversion was obtained at 225°C by Pierre *et al.* (2007).

In the study of Çağlayan and Aksoylu (2009), experiments were carried out on the bimetallic Pt-Ni/Al<sub>2</sub>O<sub>3</sub> catalyst in the 200-500°C temperature range using an idealized feed composition consisting of 3 mol% CO, 6-10 mol% H<sub>2</sub>O, and 87-91mol% inert gas. The effect of H<sub>2</sub>O/CO ratio on WGS activity was investigated using two different values, 10/3 and 2. The results showed that the effect of the H<sub>2</sub>O/CO ratio on CO conversion was similar to the effect of Ni loading. At 225°C, for a H<sub>2</sub>O/CO ratio of 2 and 5 wt.%Ni content, CO conversion was less than 5%. When the Ni content was increased to 15wt.%, CO conversion increased to about 10%. Setting the H<sub>2</sub>O/CO ratio to 10/3, roughly 5% and 15% CO conversions were obtained for 5wt.%Ni and 15wt.%Ni content, respectively.

#### 4.2. Effect of H<sub>2</sub> Addition to the Feed Stream

The basic concept of the parametric study was to observe the effect of increasing levels of H<sub>2</sub> on the activity of the 1.4wt.%Pt-5wt.%CeO<sub>x</sub>/γ-Al<sub>2</sub>O<sub>3</sub> catalyst, and experiments were performed to test the product existence effect. Table 4.2 and Figure 4.2 display the

data for WGS activity for three different H<sub>2</sub> amounts (10%, 15%, and 25% by mol) at 225°C. The CO and H<sub>2</sub>O concentrations were and kept constant at 5 mol% and 15 mol%, respectively, by adjusting the balance with N<sub>2</sub>.

Table 4.2. Effect of product H<sub>2</sub> in the feed on CO conversion at 225 °C over 1.4wt.%Pt-5wt.%CeO<sub>x</sub>/γ-Al<sub>2</sub>O<sub>3</sub> using feed with 5% CO, 15% H<sub>2</sub>O in N<sub>2</sub>

Time(min)	CO conversion (%)			
	10% H <sub>2</sub>	15% H <sub>2</sub>	25% H <sub>2</sub>	without H <sub>2</sub>
30	8,72	8,29	9,88	15,81
60	9,03	8,58	8,89	15,94
90	6,95	8,80	9,78	15,78
120	7,55	10,00	8,70	14,90
150	8,67	8,07	8,53	15,11
180	8,29	7,83	8,55	13,99

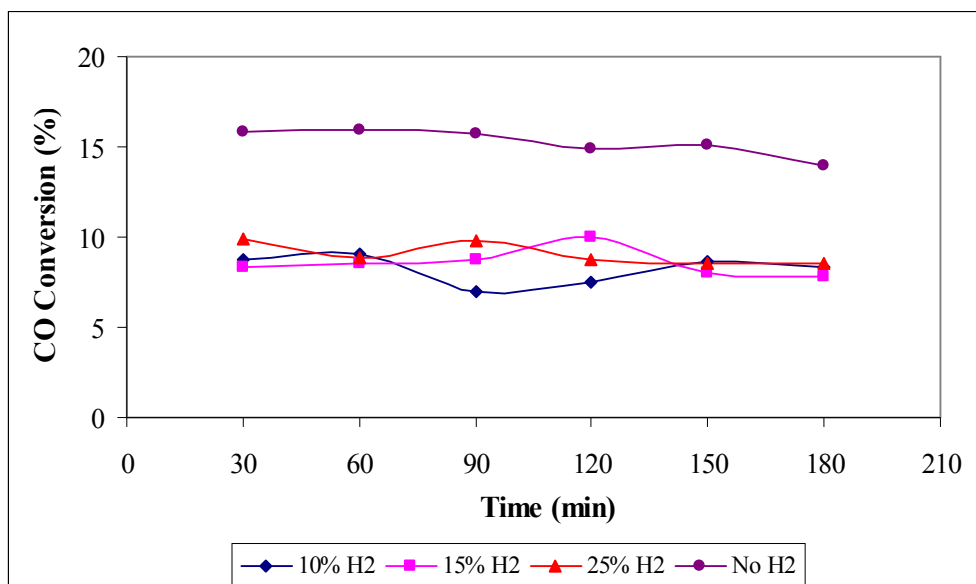


Figure 4.2. Effect of H<sub>2</sub> in feed on CO conversion at 225°C over 1.4wt.%Pt-5wt.%CeO<sub>x</sub>/γ-Al<sub>2</sub>O<sub>3</sub>

It can be inferred from Table 4.2 that increasing the H<sub>2</sub> amount from 10% to 25% does not lead to a dramatic decline in CO conversion. On the other hand, when product-

free and hydrogen containing feed streams are compared to the each other, roughly 6% of incremental decrease in CO conversion is caused by the suppressive effect of H<sub>2</sub> existence.

In the study of Evin *et al.* (2008), catalytic activity tests were performed at 200-300°C using inlet gas flows of 3.75 cm<sup>3</sup>/min CO, 62.5 cm<sup>3</sup>/min H<sub>2</sub>O and 67.5 cm<sup>3</sup>/min H<sub>2</sub>. 10%, 20%, 50% and 70% CO conversion was observed at the temperatures of 225, 250, 275 and 300°C, respectively, and the results at 225°C compare well with the present work.

### 4.3. Effect of CO<sub>2</sub> Addition to the Feed Stream

The effect of increasing levels of CO<sub>2</sub> on the catalytic activity of the particulate 1.4wt.%Pt-5wt.%CeO<sub>x</sub>/γ-Al<sub>2</sub>O<sub>3</sub> catalyst was investigated at three different CO<sub>2</sub> levels. Table 4.3 and Figure 4.3 display the CO conversions obtained at 225°C with 5%, 7.5% and 10% by mol CO<sub>2</sub> in the feed. The CO and H<sub>2</sub>O concentrations were and kept constant at 5 mol% and 15 mol%, respectively, adjusting the balance with N<sub>2</sub>.

Table 4.3. Effect of product CO<sub>2</sub> in the feed on CO conversion at 225 °C over 1.4wt.%Pt-5wt.%CeO<sub>x</sub>/γ-Al<sub>2</sub>O<sub>3</sub> using feed with 5% CO, 15% H<sub>2</sub>O in N<sub>2</sub>

Time(min)	CO conversion (%)			
	5% CO <sub>2</sub>	7.5% CO <sub>2</sub>	10% CO <sub>2</sub>	without CO <sub>2</sub>
30	15,15	15,12	10,79	15,81
60	14,40	12,03	11,03	15,94
90	13,07	11,28	8,71	15,78
120	13,84	10,69	8,60	14,90
150	13,50	10,91	8,37	15,11
180	13,83	12,04	3,60	13,99

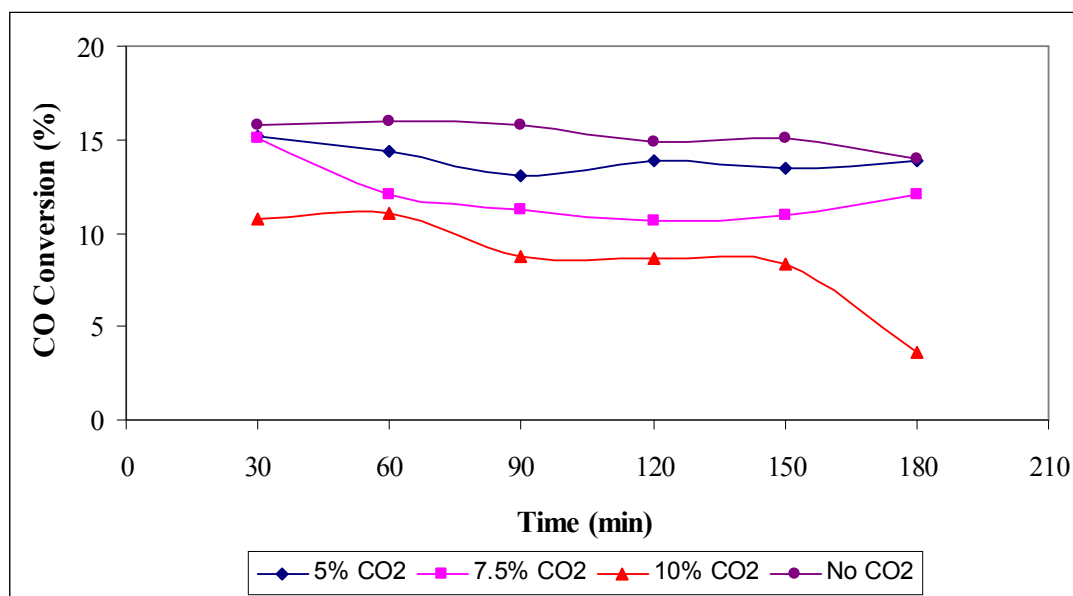


Figure 4.3. Effect of CO<sub>2</sub> in feed on CO conversion at 225°C over 1.4wt.%Pt-5wt.%CeO<sub>x</sub>/γ-Al<sub>2</sub>O<sub>3</sub>

It is evident that increasing levels of CO<sub>2</sub> in feed mixture lead to further decrease in CO conversion. Unlike the H<sub>2</sub> addition effect, approximately 2-3% incremental decrease in CO conversion is observed for 5-7.5 mol% CO<sub>2</sub> in the feed stream. The largest conversion decline is recorded for 10 mol% CO<sub>2</sub> containing stream. These results suggest that the CO<sub>2</sub> existing in the exit reformat in a fuel processor suppresses CO conversion of WGS at low temperatures. One can assume that the low desorption rate of CO<sub>2</sub> or its high surface coverage at low temperatures results in low activity at about 200°C. Tanaka *et al.* (2003) suggest that the promotion of CO<sub>2</sub> desorption at lower temperatures is one of the key issues in developing LTWGS catalysts. The material and surface modification of supports can also affect desorption of CO<sub>2</sub>.

#### 4.4. Effect of Simultaneous H<sub>2</sub> and CO<sub>2</sub> Addition to the Feed Stream

The effect of the existence of both H<sub>2</sub> and CO<sub>2</sub> on catalytic activity was also studied to mimic the typical conditions in the exit stream of the reformer unit of a fuel processor. For 1.4wt.%Pt-5wt.%CeO<sub>x</sub>/γ-Al<sub>2</sub>O<sub>3</sub> catalyst, two feed mixtures were studied by changing the steam content as follows: (5% CO, 15% H<sub>2</sub>O, 25% H<sub>2</sub>, 10%CO<sub>2</sub>) and (5% CO, 25% H<sub>2</sub>O, 25% H<sub>2</sub>, 10%CO<sub>2</sub>) at 225, 250 and 275°C to cover the temperature effect; the CO

conversions are given in Table 4.4 and Figure 4.4. Comparison of results at 225°C with those in Table 4.1 shows that CO conversion is reduced drastically to about one third. The higher H<sub>2</sub>O/CO ratio of 5 (Table 4.5 and Figure 4.5) improves CO conversion at 275°C.

Table 4.4. Effect of 25% H<sub>2</sub> and 10% CO<sub>2</sub> in the feed on CO conversion at H<sub>2</sub>O/CO=3 over 1.4wt.%Pt-5wt.%CeO<sub>x</sub>/γ-Al<sub>2</sub>O<sub>3</sub>

Time(min)	CO conversion (%)		
	225°C	250°C	275°C
30	5,05	17,86	36,7
60	5,55	16,68	41,1
90	5,99	15,46	37,45
120	5,75	13,79	35,71
150	5,2	14,07	35,24
180	5,32	14,08	32,78

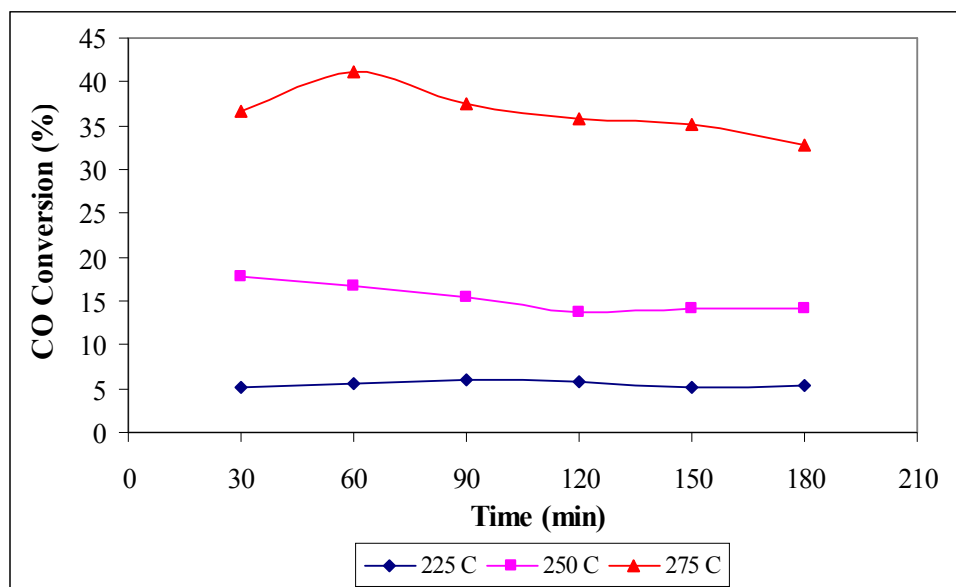


Figure 4.4. Effect of CO<sub>2</sub> and H<sub>2</sub> addition on CO conversion over 1.4wt.%Pt-5wt.%CeO<sub>x</sub>/γ-Al<sub>2</sub>O<sub>3</sub> using H<sub>2</sub>O/CO=3

In the study of Lim *et. al.* (2009), inlet gas with 6% CO, 6% CO<sub>2</sub>, 4% H<sub>2</sub>, 20% H<sub>2</sub>O, and 64% N<sub>2</sub> composition was used over 1wt.%Pt/CZO; CO conversion was not favored at all at 225°C while 7% and 17% conversions were observed at 250 and 275°C respectively.

Table 4.5. Effect of 25% H<sub>2</sub> and 10% CO<sub>2</sub> in the feed on CO conversion at H<sub>2</sub>O/CO=5 over 1.4wt.%Pt-5wt.%CeO<sub>x</sub>/γ-Al<sub>2</sub>O<sub>3</sub>

Time(min)	CO conversion (%)		
	225°C	250°C	275°C
30	6,37	21,98	48,97
60	6,84	19,7	45,39
90	5,51	20,42	41,98
120	6,2	19,81	41,38
150	5,57	18,3	41,85
180	5,55	17,73	43,71

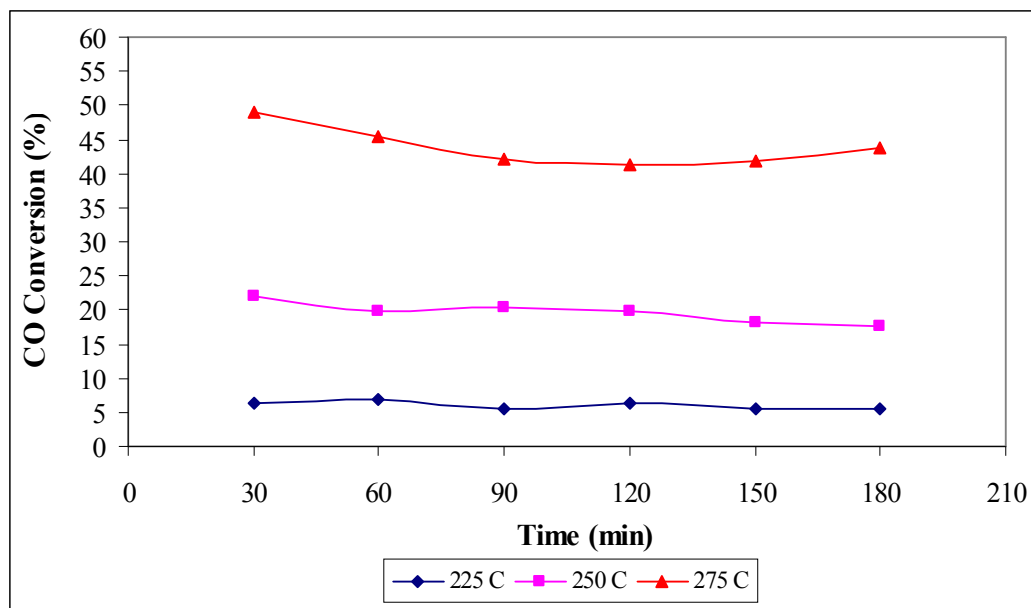


Figure 4.5. Effect of CO<sub>2</sub> and H<sub>2</sub> addition on CO conversion over 1.4wt.%Pt-5wt.%CeO<sub>x</sub>/γ-Al<sub>2</sub>O<sub>3</sub> using H<sub>2</sub>O/CO=5

Ricote and colleagues (2006) investigated inlet gas composition of 26.1% H<sub>2</sub>O, 3% CO, 29.8% H<sub>2</sub>, 11.2% CO<sub>2</sub>, 29.9% N<sub>2</sub> over the 1wt.% Pt/CeO<sub>2</sub> catalyst where the ceria support was prepared by precipitation deposition and Pt was added by incipient wetness impregnation. The CO conversions obtained at 225, 250, 275 and 300°C were 13.8%, 26%, 43.3% and 61.3%, respectively.

Sekine *et. al.* (2009) used feed consisting of (CO/H<sub>2</sub>O/H<sub>2</sub>/N<sub>2</sub>/Ar = 6/30/42/9/13) over perovskite oxides LaBO<sub>3</sub> (B = Cr, Mn, Fe, Co and Ni) prepared by the Pechini method and the Pt and Pd were loaded by impregnation. Among the perovskite-supported Pt catalysts, 1wt.%Pt/LaCoO<sub>3</sub> catalyst showed the highest activity for WGS; initial CO conversion on Pt/LaCoO<sub>3</sub> was 77%. Then, Pt/SrTiO<sub>3</sub>, Pt/LaFeO<sub>3</sub> and Pt/LaNiO<sub>3</sub> were in the second active group, whose respective initial CO conversions were 49%, 30%, and 21% at 300°C. 0.5wt.%Pd/1wt.%Pt/LaCoO<sub>3</sub> showed nearly 80% CO conversion at the same temperature.

Comparison of Table 4.5 with Table 4.6 and Figure 4.6 shows that increasing the CeO<sub>x</sub> content to 10wt.%, and testing 1.4wt.%Pt-10wt.%CeO<sub>x</sub>/γ-Al<sub>2</sub>O<sub>3</sub> in mixed feed with H<sub>2</sub>O/CO ratio of 5 between 225-275 °C has a minor effect only at the lower temperatures.

Table 4.6. Effect of 25% H<sub>2</sub> and 10% CO<sub>2</sub> in the feed on CO conversion at H<sub>2</sub>O/CO=5 over 1.4wt.%Pt-10wt.%CeO<sub>x</sub>/γ-Al<sub>2</sub>O<sub>3</sub>

Time(min)	CO conversion (%)		
	225°C	250°C	275°C
30	8,05	23,61	46,02
60	8,88	22,72	43,18
90	10,23	24,13	43,16
120	8,58	24,25	41,3
150	8,02	21,87	41,7
180	8,37	22,66	42,68

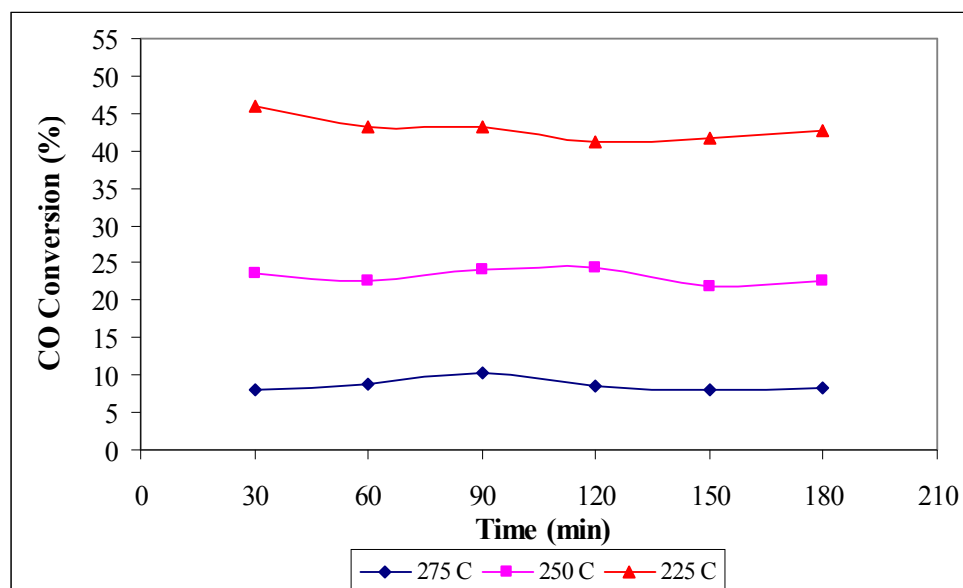


Figure 4.6. Effect of CO<sub>2</sub> and H<sub>2</sub> addition on CO conversion over 1.4wt.%Pt-10wt.%CeO<sub>x</sub>/γ-Al<sub>2</sub>O<sub>3</sub> using H<sub>2</sub>O/CO=5

Bera *et. al.* (2004), have studied catalysts prepared by combustion synthesis method, and among catalysts tested at 125-200°C, 2wt.%Pt-CeO<sub>2</sub> gave higher CO conversion than 1wt.%Pt-CeO<sub>2</sub>. The feed composition was 5% CO, 40% H<sub>2</sub>, 10% CO<sub>2</sub> and 1% CH<sub>4</sub>. At 200°C, 90% of CO is converted over 2wt.% Pt/CeO<sub>2</sub> whereas approximately 80% CO conversion is achieved by 1wt.% Pt/CeO<sub>2</sub>.

The monolithic catalyst prepared in this study targeting 1.4wt.%Pt-5wt.%CeO<sub>x</sub> loading on the alumina wash-coat was also tested for its LTWGS performance. Tests were carried out with both pure (5% CO, 15% H<sub>2</sub>O) and realistic feed mixtures (5% CO, 15% H<sub>2</sub>O, 25% H<sub>2</sub>, 10% CO<sub>2</sub>) by adjusting N<sub>2</sub> as a balance at the temperatures of 250, 275 and 300°C (Tables 4.7 and 4.8; Figures 4.7 and 4.8). In the light of CO conversion values of monolithic catalysts at 250 and 275°C, it was concluded that there was no need for an experiment at 225°C. Here 300°C was chosen to find the temperature at which CO conversion is comparable to the particulate catalyst. Monolithic catalysts are reported to require higher temperatures than particulate catalysts of similar composition. Inductively Coupled Plasma (ICP) analysis by TÜBİTAK showed that 39% of the targeted Pt was actually deposited on alumina wash-coated monoliths.

Table 4.7. CO conversion over 1.4wt.%Pt-5wt.%CeO<sub>x</sub>/γ-Al<sub>2</sub>O<sub>3</sub> monolithic catalyst with pure feed using H<sub>2</sub>O/CO=3

Time(min)	CO conversion (%)		
	250°C	275°C	300°C
30	6,95	15,57	33,29
60	6,64	14,70	32,38
90	7,93	14,28	31,16
120	6,63	15,26	31,00
150	6,56	15,01	29,78
180	6,76	14,36	29,80

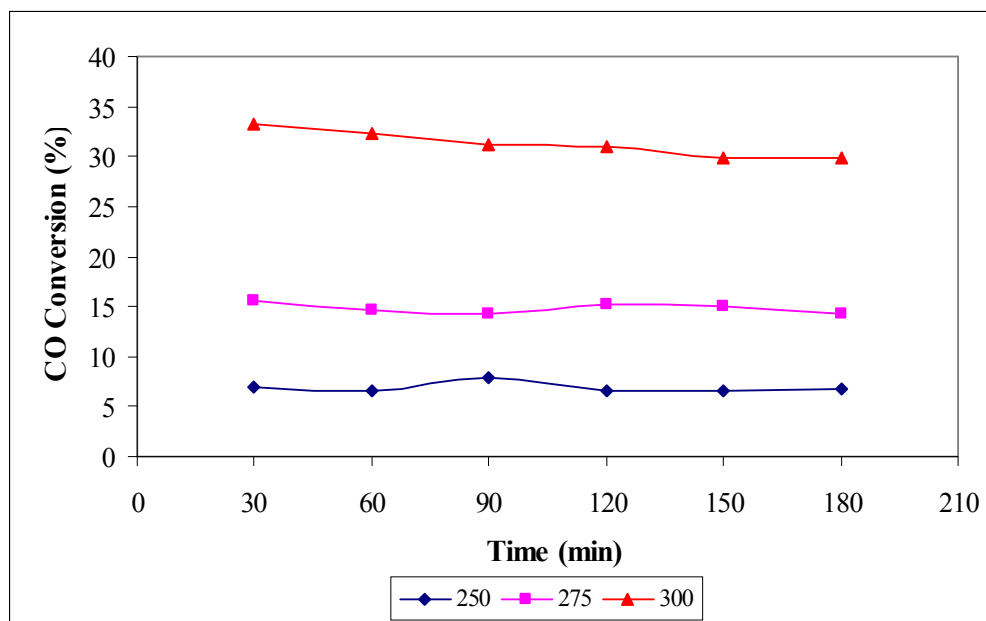


Figure 4.7. Effect of temperature on CO conversion over 1.4wt.%Pt-5wt.%CeO<sub>x</sub>/γ-Al<sub>2</sub>O<sub>3</sub> monolithic catalyst using pure feed and H<sub>2</sub>O/CO=3

Table 4.8. CO conversion over 1.4wt.%Pt-5wt.%CeO<sub>x</sub>/γ-Al<sub>2</sub>O<sub>3</sub> monolithic catalyst using mixed feed with CO<sub>2</sub> and H<sub>2</sub> at H<sub>2</sub>O/CO=3

Time(min)	CO conversion (%)		
	250°C	275°C	300°C
30	4,16	4,1	15,09
60	4,78	5,04	14,72
90	4,61	6,01	15,13
120	4,45	5,79	14,74
150	3,89	5,29	14,79
180	4,13	5,09	14,66

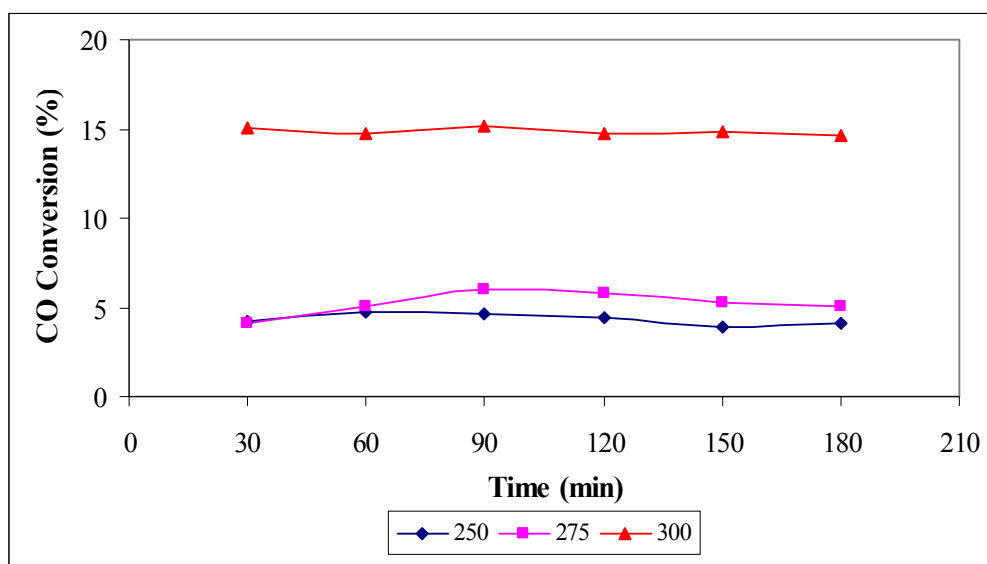


Figure 4.8. Effect of temperature on CO conversion over 1.4wt.%Pt-5wt.%CeO<sub>x</sub>/γ-Al<sub>2</sub>O<sub>3</sub> monolithic catalyst using mixed feed with CO<sub>2</sub> and H<sub>2</sub> at H<sub>2</sub>O/CO=3

Table 4.7 indicates that increasing the temperature from 250 to 275°C doubles the CO conversion of about 7% to over 14%; increase in temperature from 275 to 300°C further doubles the CO conversion to 30%. The CO conversion attained at 300°C is close to the ca. 33% CO conversion at 275°C over the particulate catalyst (Table 4.4).

The existence of products in the feed stream suppresses CO conversion in comparison to experiment carried out using pure feed, as expected. It is interesting that the conversion difference between the pure and mixed feed is about 2-3% at 250°C and 180 min time-on-stream, while at 275°C this difference is drastic and reduces the pure feed conversion of ca. 15% down to 5%. Similarly, the introduction of products into the feed at 300°C pulls down CO conversion from ca. 30% to ca. 15%. It is worth noting that the mixed feed CO conversions of 300°C are at the same level as the pure feed CO conversion values of 275°C.

In the study of Du and colleagues (2008),  $\text{Ce}_{0.8}\text{Zr}_{0.2}\text{O}_2$  slurry was prepared by wet ball milling and cordierite substrates were coated by dipping into  $\text{Ce}_{0.8}\text{Zr}_{0.2}\text{O}_2$  slurry. The active metals were loaded by submerging the  $\text{Ce}_{0.8}\text{Zr}_{0.2}\text{O}_2$  coated substrate into Pt or Re salt solution. Experiments were performed using the dry feed gas composition as 56%  $\text{H}_2$ , 3.4% CO, 22%  $\text{CO}_2$  and  $\text{N}_2$  balance with a steam/dry gas molar ratio of 0.25 over 0.34wt.%Pt and 1wt.%Pt containing 50wt.% $\text{Ce}_{0.8}\text{Zr}_{0.2}\text{O}_2$ /cordierite catalyst. Approximately 20%, 40%, 60% CO conversions were observed at 225, 250 and 275°C, respectively, for the 0.34wt.%Pt catalyst. On the other hand, roughly 36%, 61%, 65% CO conversions were observed at 225, 250 and 275°C, respectively, for the 1wt.%Pt catalyst.

The effect of different Pt/Re additions (1:1, 3:1, 3:2, 6:1) on 0.34wt.%Pt containing 50wt.% $\text{Ce}_{0.8}\text{Zr}_{0.2}\text{O}_2$ /cordierite catalyst were also investigated by the same group. Pt/Re=3:1 gave the highest conversions among the various compositions studied. Around 45%, 68%, 65% CO conversions were observed at 225, 250 and 275°C, respectively (Du *et. al.*, 2008).

As the realistic scenario, WGS performances of particulate and monolithic catalysts are compared in Table 4.9 and Figure 4.9 at 250 and 275°C using mixed feed with  $\text{CO}_2$  and  $\text{H}_2$  at a  $\text{H}_2\text{O}/\text{CO}$  ratio of 3. The temperature increase is significant for the particulate catalyst but not for the monolith catalyst.

Table 4.9. Comparison of CO conversions over particulate and monolithic Pt-CeO<sub>x</sub> catalysts using mixed feed with CO<sub>2</sub> and H<sub>2</sub> at H<sub>2</sub>O/CO=3

Time (min)	Particulate		Monolith	
	275	250	275	250
30	36,70	17,86	4,10	4,16
60	41,10	16,68	5,04	4,78
90	37,45	15,46	6,01	4,61
120	35,71	13,79	5,79	4,45
150	35,24	14,07	5,29	3,89
180	32,78	14,08	5,09	4,13

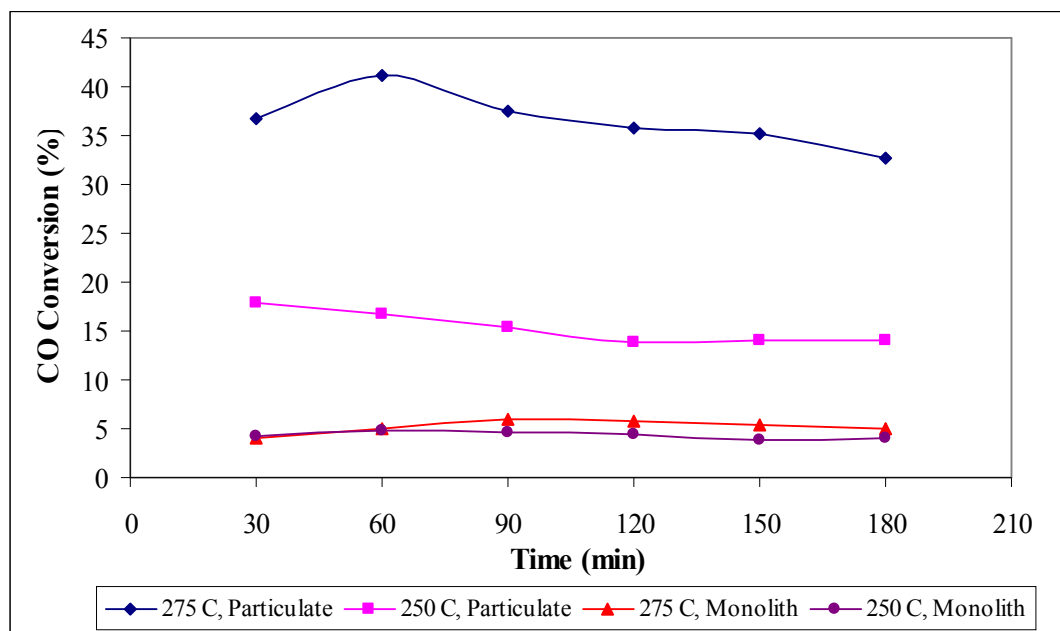


Figure 4.9. Effect of Pt-CeO<sub>x</sub> catalyst type on CO conversion using realistic mixed feed with CO<sub>2</sub> and H<sub>2</sub> at H<sub>2</sub>O/CO=3

The equilibrium conversions calculated for realistic feed mixtures with CO<sub>2</sub> and H<sub>2</sub> at H<sub>2</sub>O/CO ratios of 3 and 5 are compared with CO conversions obtained over particulate 1.4wt.%Pt-5wt.%CeO<sub>x</sub>/γ-Al<sub>2</sub>O<sub>3</sub> catalyst in Figures 4.10 and 4.11, respectively.

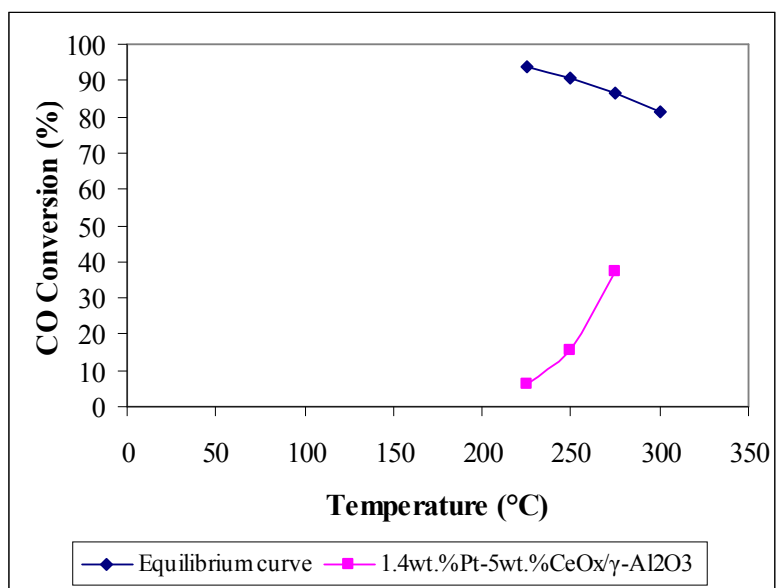


Figure 4.10. Comparison of CO conversions over 1.4wt.%Pt-5wt.%CeO<sub>x</sub>/γ-Al<sub>2</sub>O<sub>3</sub> with equilibrium data using mixed feed with CO<sub>2</sub> and H<sub>2</sub> at H<sub>2</sub>O/CO=3 (90 min time-on-stream)

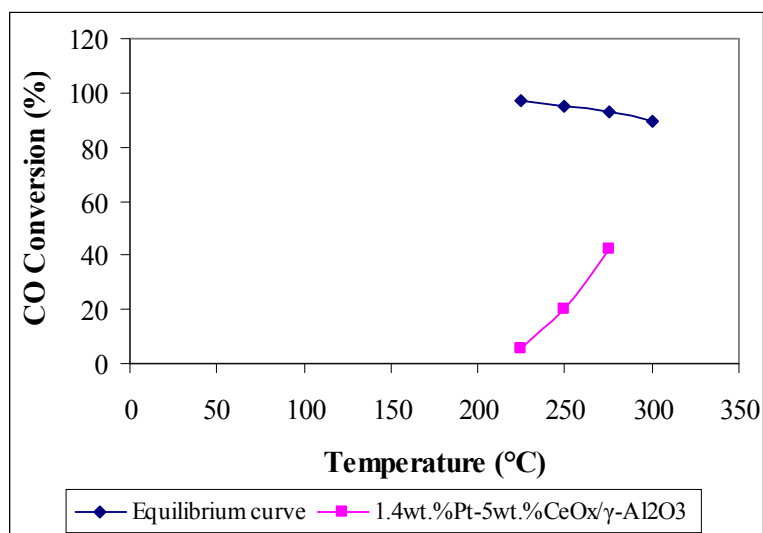


Figure 4.11. Comparison of CO conversions over 1.4wt.%Pt-5wt.%CeO<sub>x</sub>/γ-Al<sub>2</sub>O<sub>3</sub> with equilibrium data using mixed feed with CO<sub>2</sub> and H<sub>2</sub> at H<sub>2</sub>O/CO=5 (90 min time-on-stream)

Similar CO conversion data obtained over the alumina wash-coated monolithic Pt-CeO<sub>x</sub> catalyst using feed mixtures with CO<sub>2</sub> and H<sub>2</sub> at a H<sub>2</sub>O/CO ratio of 5 are compared with equilibrium data in Figure 4.12. The equilibrium CO conversions of mixed feed containing 5%CO, 15% or 25% H<sub>2</sub>O, 25% H<sub>2</sub> and 10% CO<sub>2</sub> with inert N<sub>2</sub> as balance were

calculated using computer software HSC4 (HSC Chemistry Version 4.1, Outokumpu Research Oy.) Comparisons in Figures 4.10-4.12 clearly indicate that the CO conversions achieved over particulate and monolithic Pt-CeO<sub>x</sub> catalysts used in this study are well below equilibrium CO conversions at the corresponding LTWGS temperatures, and there is room for improvement in catalyst design to speed up the rate of approach to equilibrium at temperatures in the 200-300°C range.

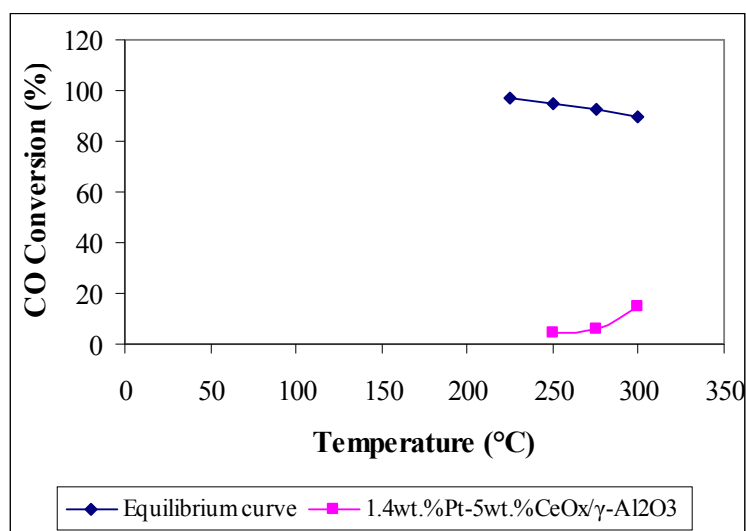


Figure 4.12. Comparison of CO conversions over monolithic Pt-CeO<sub>x</sub> catalyst with equilibrium data using mixed feed with CO<sub>2</sub> and H<sub>2</sub> at H<sub>2</sub>O/CO=3 (90 min time-on-stream)

## 5. CONCLUSIONS AND RECOMMENDATIONS

### 5.1. Conclusions

The low temperature water gas shift (LTWGS) reaction was studied on Pt-ceria catalysts supported over particulate and monolithic structures using both pure and realistic mixed feed compositions in the 225-300°C temperature range. The LTWGS reaction was carried out using three different catalysts, particulate 1.4wt.%Pt-5wt.%CeO<sub>x</sub>/γ-Al<sub>2</sub>O<sub>3</sub> and 1.4wt.%Pt-10wt.%CeO<sub>x</sub>/γ-Al<sub>2</sub>O<sub>3</sub> and monolithic 1.4wt.%Pt-5wt.%CeO<sub>x</sub>/γ-Al<sub>2</sub>O<sub>3</sub>. Effects of H<sub>2</sub>O/CO ratio, H<sub>2</sub> or CO<sub>2</sub> addition to the feed, simultaneous addition of H<sub>2</sub> and CO<sub>2</sub> to the feed, reaction temperature and cerium oxide loading on CO conversion were investigated. Particulate catalysts were prepared by sequential incipient-to-wetness impregnation while alumina wash-coated monolithic catalysts were prepared by co-impregnation.

The major conclusions obtained in this study can be summarized as follows:

- CO conversion increases from 7.5% to 27% as H<sub>2</sub>O/CO ratio is increased from 1 to 7, and the most significant enhancement is observed at ratios of 2 and 5.
- Reaction temperature has a significant effect on CO conversion over all the catalysts studied. CO conversion over particulate 1.4wt.%Pt-5wt.%CeO<sub>x</sub>/γ-Al<sub>2</sub>O<sub>3</sub> increases as reaction temperature is increased from 225 to 275°C; similar results are obtained over monolithic 1.4wt.%Pt-5wt.%CeO<sub>x</sub> as temperature is increased from 250 to 300°C.
- Addition of 25 mol% H<sub>2</sub> product into the feed at 225°C and a H<sub>2</sub>O/CO ratio of 3 decreases CO conversion from 15-16% to 9%. Addition of 10 mol% CO<sub>2</sub> product into the feed at 225°C and a H<sub>2</sub>O/CO ratio of 3 leads to a similar decrease up to 150 minutes time-on-stream after which the CO conversion drops down to 4%.
- The simultaneous addition of 25 mol% H<sub>2</sub> and 10 mol% CO<sub>2</sub> at 225°C using H<sub>2</sub>O/CO ratios of 3 or 5 lowers CO conversion to 5-6%. Similar experiments at 250 and 275°C show that temperature has a significant effect on CO conversion; the highest value of CO conversion at 275°C is ca. 33% with a H<sub>2</sub>O/CO ratio of 3 and 44% with a H<sub>2</sub>O/CO ratio of 5, both at 180 minutes time-on-stream.

- The difference in catalytic activities of particulate 1.4wt.%Pt-10wt.%CeO<sub>x</sub>/γ-Al<sub>2</sub>O<sub>3</sub> and 1.4wt.%Pt-5wt.%CeO<sub>x</sub>/γ-Al<sub>2</sub>O<sub>3</sub> catalysts under realistic feed mixtures with CO<sub>2</sub> and H<sub>2</sub> is not significant, which is consistent with pure feed comparisons.
- Tests conducted with the monolithic catalyst targeting 1.4wt.%Pt-5wt.%CeO<sub>x</sub> loading on alumina wash-coat at 250, 275 and 300°C using both pure and mixed feed at a H<sub>2</sub>O/CO ratio of 3 confirm that monolithic catalysts require higher temperatures than particulate catalysts having similar composition. The highest CO conversion attained over the monolith at 300°C was 30% with pure feed and 15% with mixed feed, while the corresponding conversions over the particulate catalyst in mixed feed were about 15% at 250°C and 35% at 275°C.
- CO conversions achieved over alumina-supported particulate and monolithic Pt-ceria catalysts used in this work are well below equilibrium CO conversions calculated at the corresponding LTWGS temperatures.

## 5.2. Recommendations

Based on the experimental results, the following recommendations can be made for future studies on the WGS reaction over alumina-supported Pt-ceria catalysts:

- Kinetic experiments may be conducted for finding an empirical kinetic expression for low-temperature water-gas shift reaction over particulate Pt-CeO<sub>x</sub>/γ-Al<sub>2</sub>O<sub>3</sub> catalyst.
- Physical properties of the catalysts such as BET surface area, XRD patterns and SEM images may be obtained to study the interaction between Pt and CeO<sub>x</sub> components of the Pt-CeO<sub>x</sub>/γ-Al<sub>2</sub>O<sub>3</sub> catalyst in detail in order to improve catalyst design.
- Same catalysts and feed conditions can be applied to study the HTWGS reaction.

## APPENDIX A: THE LIST OF EXPERIMENTS PERFORMED OVER LOW TEMPERATURE WATER GAS SHIFT REACTION

The list of experiments performed over LWGSR is given in Table A.1.

Exp .No	Total Flow Rate (ml/min)	Metal Composition (wt.%)		Temperature (°C)	Feed Gas Composition (Balance with He)			
		Pt	Ce		CO	H <sub>2</sub> O	H <sub>2</sub>	CO <sub>2</sub>
1	100	1.4	5	225	5	5	0	0
2	100	1.4	5	225	5	10	0	0
3	100	1.4	5	225	5	15	0	0
4	100	1.4	5	225	5	25	0	0
5	100	1.4	5	225	5	35	0	0
6	100	1.4	5	225	5	15	10	0
7	100	1.4	5	225	5	15	15	0
8	100	1.4	5	225	5	15	25	0
9	100	1.4	5	225	5	15	0	5
10	100	1.4	5	225	5	15	0	7.5
11	100	1.4	5	225	5	15	0	10
12	100	1.4	5	225	5	15	25	10
13	100	1.4	5	250	5	15	25	10
14	100	1.4	5	275	5	15	25	10
15	100	1.4	5	225	5	25	25	10
16	100	1.4	5	250	5	25	25	10
17	100	1.4	5	275	5	25	25	10
18	100	1.4	10	225	5	25	25	10
19	100	1.4	10	250	5	25	25	10
20	100	1.4	10	275	5	25	25	10
21	100	1.4	5	250	5	15	0	0
22	100	1.4	5	275	5	15	0	0
23	100	1.4	5	300	5	15	0	0
24	100	1.4	5	250	5	15	25	10
25	100	1.4	5	275	5	15	25	10
26	100	1.4	5	300	5	15	25	10

## REFERENCES

- Adams, W. A., J. Blair, K. R. Bullock and C. L. Gardner, 2005, "Enhancement of the Performance and Reliability of CO Poisoned PEM Fuel Cells", *Journal of Power Sources*, Vol. 145, pp. 55-61.
- Ahmed S., M. Krumpelt, 2001, "Hydrogen from hydrocarbon fuels for fuel cells", *International Journal of Hydrogen Energy*, Vol. 26, pp. 291-301.
- Anderson, J. R., M. Boudart, 1982, *Catalysis Science and Technology*, Springer-Verlag, Berlin Heidelberg, New York.
- Andreeva D., V. Idakiev, T. Tabakova, L. Ilieva, P. Falaras, A. Bourlinos and A. Travlos, 2002, "Low-temperature water-gas shift reaction over Au/CeO<sub>2</sub> catalysts", *Catalysis Today*, Vol. 72, pp. 51-57.
- Araújo G. C. and M. C. Rangel, 2000, "An environmental friendly dopant for the high-temperature shift catalysts", *Catalysis Today*, Vol. 62, pp. 201-207.
- Avcı A. K., D. L. Trimm and Z. İ. Önsan, 2002, "Quantitative investigation of catalytic natural gas conversion for hydrogen fuel cell applications", *Chemical Engineering Journal*, Vol. 90, pp. 77-87.
- Avcı A. K., Z. İ. Önsan and D. L. Trimm, 2001, "On-board fuel conversion for hydrogen fuel cells: comparison of different fuels by computer simulations", *Applied Catalysis A: General*, Vol. 216, pp. 243-256.
- Ayabe S., H. Omoto, T. Utaka, R. Kikuchi, K. Sasaki, Y. Teraoka and K. Eguchi, 2003, "Catalytic autothermal reforming of methane and propane over supported metal catalysts", *Applied Catalysis A: General*, Vol. 241, pp. 261-269.

- Azzam, K. G., I. V. Babich, K. Seshan and L. Lefferts, 2007, "A Bifunctional Catalyst for the Single-Stage Water-Gas Shift Reaction in Fuel Cell Applications: Part 2. Roles of the Support and Promoter on Catalyst Activity and Stability", *Journal of Catalysis*, Vol. 251, pp. 163-171.
- Badmaev S. D. and P. V. Snytnikov, 2008, "Hydrogen production from dimethyl ether and bioethanol for fuel cell applications", *International Journal of Hydrogen Energy*, Vol. 33, pp. 3026-3030.
- Barbir F. (editor), 2005, *PEM Fuel Cells*, Elsevier Academic Press, London.
- Basinska, A. and F. Domka, 1999, "The Effect of Lanthanides on the Ru/Fe<sub>2</sub>O<sub>3</sub> Catalysts for Water-Gas Shift Reaction", *Applied Catalysis A: General*, Vol. 179, pp. 241-246.
- Bera P., S. Malwadkar, A. Gayen, C.V.V. Satyanarayana, B.S. Rao and M.S. Hegde, 2004, "Low-temperature water gas shift reaction on combustion synthesized Ce<sub>1-x</sub>Pt<sub>x</sub>O<sub>2-δ</sub> catalyst", *Catalysis Letters*, Vol. 96, pp. 213-219.
- Boettner, D. D. and M. J. Moran, 2004, "Proton Exchange Membrane (PEM) Fuel Cell-Powered Vehicle Performance Using Direct-Hydrogen Fueling and On-Board Methanol reforming", *Energy*, Vol. 29, pp. 2317-2330.
- Bohlbro H. (editor), 1969, *Investigation on Kinetics of the Conversion of Carbon Monoxide with Water Vapour over Iron Oxide Based Catalysts*, Haldor Topsoe Research Laboratory, Copenhagen, 2nd ed., pp 6.
- Brown, L. F., 2001, "A Comparative Study of Fuels for On-Board Hydrogen Production for Fuel-Cell-Powered Automobiles", *International Journal of Hydrogen Energy*, Vol. 26, pp. 381-397.
- Brunetti A., G. Barbieri and E. Drioli, 2008, "A PEMFC and H<sub>2</sub> membrane purification integrated plant" *Chemical Engineering and Processing*, Vol. 47, pp. 1081-1089.

- Buxbaum R. and H. Lei, 2003, "Power output and load in a fuel cell fueled by membrane reactor hydrogen", *Journal of Power Sources*, Vol. 123, pp. 43-47.
- Chan S.H. and H.M. Wang, 2000, "Thermodynamic analysis of natural-gas fuel processing for fuel cell applications", *International Journal of Hydrogen Energy*, Vol. 25, pp. 441-449.
- Chen W.H., T.C. Hsieh and T.L. Jiang, 2008, "An experimental study on carbon monoxide conversion and hydrogen generation from water gas shift reaction", *Energy Conversion and Management*, Vol. 49, pp. 2801-2808.
- Cindrella L., A.M. Kannan, J.F. Lin, K. Saminathan, Y. Ho, C.W. Lin and J. Wertz, 2009, "Gas Diffusion Layer for Proton Exchange Membrane Fuel Cells – a Review", *Journal of Power Sources*, In Press.
- Cipití F., L. Pino, A. Vita, M. Laganà and V. Recupero, 2008, "Performance of a 5 kW<sub>e</sub> fuel processor for polymer electrolyte fuel cells" *International Journal of Hydrogen Energy*, Vol. 33, pp. 3197-3203.
- Costa J. L. R., G. S. Marchetti and M. C. Rangel, 2002, "A thorium-doped catalyst for the high temperature shift reaction", *Catalysis Today*, Vol. 77, pp. 205-213.
- Çağlayan B. S. and A. E. Aksoylu, 2009, "Water-Gas Shift Reaction over Bimetallic Pt-Ni/Al<sub>2</sub>O<sub>3</sub> Catalysts", *Turkish Journal of Chemistry*, Vol. 33, pp. 249-256.
- Diwell, A. F., R. R. Rajaram, H. A. Shaw, T. J. Truex, 1991, "The Role of Ceria in Three-Way Catalysts", in *Catalysis and Automotive Pollution Control II*; A. Cruq (Editor), Elsevier Science Publishers B.V. Amsterdam, The Netherlands, Vol. 71, pp. 139-152.
- Döker, Y. A., 2008, "Preparation of Catalytic Cordierite Monoliths for the Selective Oxidation of Carbon Monoxide", M. S. Thesis, Boğaziçi University, Istanbul.

- Du X., D. Gao, Z. Yuana, N. Liua, C. Zhanga and S. Wang, 2008, "Monolithic Pt/Ce<sub>0.8</sub>Zr<sub>0.2</sub>O<sub>2</sub>/cordierite catalysts for low temperature water gas shift reaction in the real reformat", *International Journal of Hydrogen Energy*, Vol. 33, pp. 3710-3718.
- Evin H. N., G. Jacobs, J. Ruiz-Martinez, G. Thomas and B. H. Davis, 2008, "Low Temperature Water-Gas Shift: Alkali Doping to Facilitate Formate C-H Bond Cleaving over Pt/Ceria Catalysts—An Optimization Problem", *Catalysis Letters*, Vol. 120, pp. 166-178.
- Farias A. M. D., A. P. M. G. Barandas, R. F. Perez and M. A. Fraga, 2007, "Water-gas shift reaction over magnesia-modified Pt/CeO<sub>2</sub> catalysts", *Journal of Power Sources* Vol. 165, pp. 854–860.
- Farias A. M. D., P. Bargiela, M. G. C. Rocha, M. A. Fraga, 2008, "Vanadium-promoted Pt/CeO<sub>2</sub> catalyst for water-gas shift reaction", *Journal of Catalysis* Vol. 260 pp. 93–102.
- Farrauto R., S. Hwang, L. Shore, W. Ruettinger, J. Lampert, T. Giroux, Y. Liu and O. Ilinich, 2003, "New material needs for hydrocarbon fuel processing: Generating hydrogen for the PEM fuel cell", *Annual Review of Materials Research*, Vol. 33, pp. 1-27.
- Ferng Y. M., Y. C. Tzang, B.S. Pei, C. C. Sun and A. Su, 2004, "Analytical and experimental investigations of a proton exchange membrane fuel cell", *International Journal of Hydrogen Energy*, Vol. 29, pp. 381-391.
- Fu Q., W. Deng, H. Saltsburg and M. Flytzani-Stephanopoulos, 2005, "Activity and stability of low-content gold-cerium oxide catalysts for the water-gas shift reaction", *Applied Catalysis B: Environmental*, Vol. 56, pp. 57-68.
- Gandhia H.S. and M. Shelefa, 1987, "The Role of Research in the Development of New Generation Automotive Catalysts", *Studies in Surface Science and Catalysis*, Vol. 30, pp. 199-214.

- Gerbec M., V. Jovan and J. Petrovčić, 2008, "Operational and safety analysis of a commercial PEMFC system", *International Journal of Hydrogen Energy*, Vol. 33, pp. 4147-4160.
- Giroux T., S. Hwang, Y. Liu, W. Ruettinger and L. Shore, 2005, "Monolithic structures as alternatives to particulate catalysts for the reforming of hydrocarbons for hydrogen generation, *Applied Catalysis B: Environmental*, Vol. 56 pp. 95-110.
- Goguet A., F. Meunier, J. P. Breen, R. Burch, M. I. Petch and A. F. Ghenciu, 2004, "Study of the origin of the deactivation of a Pt/CeO<sub>2</sub> catalyst during reverse water gas shift (RWGS) reaction", *Journal of Catalysis*, Vol. 226, pp. 382-92.
- Gorte R. J. and S. Zhao, 2005, "Studies of the water-gas-shift reaction with ceria-supported precious metals, *Catalysis Today*, Vol.104, pp. 18-24.
- Guo P. J., L. F. Chen, G.B. Yu, Y. Zhu, M. H. Qiao, H. L. Xu, K. N. Fan, 2009, "Cu/ZnO-based water-gas shift catalysts in shut-down/start-up operation", *Catalysis Communications*, Vol. 10, pp. 1252-1256.
- Hagh B. F., 2003, "Optimization of autothermal reactor for maximum hydrogen production", *International Journal of Hydrogen Energy*, Vol. 28, pp. 1369-1377.
- Heck R. M., S. Gulati and R. J. Farrauto, 2001, "The application of monoliths for gas phase catalytic reactions", *Chemical Engineering Journal*, Vol. 82, pp.149-156.
- Hu Y., H. Jin, J. Liu and D. Hao, 2000, "Reactive behaviors of iron-based shift catalyst promoted by ceria", *Chemical Engineering Journal*, Vol. 78, pp. 147-152.
- Hua N., H. Wang, Y. Du, M. Shen and P. Yang, 2005, "Ultrafine Ru and  $\gamma$ -Fe<sub>2</sub>O<sub>3</sub> particles supported on MgAl<sub>2</sub>O<sub>4</sub> spinel for water-gas shift reaction", *Catalysis Communications* Vol. 6, pp. 491-496.

- Holmen A., 2009, "Direct conversion of methane to fuels and chemicals", *Catalysis Today*, Vol. 142, pp. 2–8.
- Iida, H. and A. Igarashi, 2006, "Difference in the Reaction Behavior Between Pt-Re/TiO<sub>2</sub> (Rutile) and Pt-Re/ZrO<sub>2</sub> Catalysts for Low-Temperature Water Gas Shift Reactions", *Applied Catalysis A: General*, Vol. 303, pp. 48-55.
- Iida, H., K. Kondo, A. Igarashi, 2006, "Effect of Pt Precursors on Catalytic Activity of Pt/TiO<sub>2</sub> (rutile) for Water-Gas Shift Reaction at Low-Temperature", *Catalysis Communications*, Vol. 7, pp. 240-244.
- Jacobs, G., U. M. Graham, E. Chenu, P. M. Patterson, A. Dozier and B. H. Davis, 2005b, "Low-Temperature Water-Gas Shift: Impact of Pt Promoter Loading on the Partial Reduction of Ceria and Consequences for Catalyst Design", *Journal of Catalysis*, Vol. 229, pp. 499-512.
- Joensen F., J. R. Rosstrup-Nielsen, 2002, "Conversion of hydrocarbons and alcohols for fuel cells", *Journal of Power Source*, Vol. 105, pp. 195-201.
- Juan A. M. H, C. M. Y. Yeung, S. C. Tsang, 2008, "A study of co-precipitated bimetallic gold catalysts for water–gas shift reaction", *Catalysis Communications*, Vol. 9, pp. 1551-1557.
- Kappen P., J. D. Grunwaldt, B. S. Hammershøi, L. Tröger and B. S. Clausen, 2001, "The State of Cu Promoter Atoms in High-Temperature Shift Catalysts-An in Situ Fluorescence XAFS Study", *Journal of Catalysis*, Vol. 198, pp. 56–65.
- Keiski R. L. and T. Salmi, 1992, "Deactivation of the high-temperature water-gas shift catalyst in non-isothermal conditions", *Applied Catalysis A: General*, Vol. 87, pp. 185-203.

- Kim Y. T., E. D. Park, H. C. Lee, D. Lee and K. H. Lee, 2009, "Water-gas shift reaction over supported Pt-CeO<sub>x</sub> catalysts", *Applied Catalysis B: Environmental*, Vol. 90, pp. 45-54.
- Krumpelt M., T. R. Krause, J. D. Carter, J. P. Kopasz and S. Ahmed, 2002, "Fuel processing for fuel cell systems in transportation and portable power applications" *Catalysis Today*, Vol. 77, pp. 3-16.
- Kundu M. L., A. C. Sengupta, G. C. Maiti, B. Sen, S. K. Ghosh, V. I. Kuznetsov, G. N. Kustova and E. N. Yurchenko, 1988, "Characterization of chromia-promoted  $\gamma$ -iron oxide catalysts and their CO conversion efficiency", *Journal of Catalysis*, Vol. 112, pp. 375-383.
- Ladebeck J. and K. Kochloefl, 1995, "Cr-free iron-catalysts for water-gas shift reaction", *Studies in Surface Science and Catalysis*, Vol. 91, pp. 1079-1083.
- Leppelt, R., B. Schumacher, V. Plzak, M. Kinne, R. J. Behm, 2006, "Kinetics and Mechanism of the Low-Temperature Water-Gas Shift Reaction on Au/CeO<sub>2</sub> Catalysts in an Idealized Reaction Atmosphere", *Journal of Catalysis*, Vol. 244, pp. 137-152.
- Li Y., Q. Fu and M. Flytzani-Stephanopoulos, 2000, "Low-temperature water-gas shift reaction over Cu- and Ni-loaded cerium oxide catalysts", *Applied Catalysis B: Environmental*, Vol. 27, pp. 179-191.
- Lim S., J. Bae and K. Kim, 2009, "Study of activity and effectiveness factor of noble metal catalysts for water-gas shift reaction", *International Journal of Hydrogen Energy*, Vol. 34, pp. 870-876.
- Liu Q., W. Ma, R. He and Z. Mu, 2005, "Reaction and characterization studies of an industrial Cr-free iron-based catalyst for high-temperature water gas shift reaction", *Catalysis Today*, Vol. 106, pp. 52-56.

- Lloyd L., D. E. Ridler, M. V. Twigg, (editors), 1996, *Catalysis Handbook*, Wolfe Scientific Books, London, pp.339.
- Lucrédio A F., G. T. Filho and E. M. Assaf, 2009, “Co/Mg/Al hydrotalcite-type precursor, promoted with La and Ce, studied by XPS and applied to methane steam reforming reactions”, *Applied Surface Science*, Vol. 255, pp. 5851-5856.
- Luengnaruemitchai A., S. Osuwan and E. Gulari, 2003, “Comparative studies of low-temperature water–gas shift reaction over Pt/CeO<sub>2</sub>, Au/CeO<sub>2</sub> and Au/Fe<sub>2</sub>O<sub>3</sub> catalysts”, *Catalysis Communications* Vol. 4, pp. 215-221.
- Martos C. J., Dufour and A. Ruiz, 2008, “Synthesis of Fe<sub>3</sub>O<sub>4</sub>-based catalysts for the high-temperature water gas shift reaction”, *International Journal of Hydrogen Energy*, In Press.
- Nagai M., A. M. Zahidul and K. Matsuda, 2006, “Nano-structured nickel–molybdenum carbide catalyst for low-temperature water-gas shift reaction”, *Applied Catalysis A: General*, Vol. 313, pp. 137-145.
- Nagai M. and K. Matsuda, 2006, “Low-temperature water–gas shift reaction over cobalt–molybdenum carbide catalyst”, *Journal of Catalysis*, Vol. 238, pp. 489-496.
- Natesakhawat S., X. Wang, L. Zhang, U. S. Ozkan, 2006, “Development of chromium-free iron-based catalysts for high-temperature water-gas shift reaction”, *Journal of Molecular Catalysis A: Chemical*, Vol. 260, pp. 82-94.
- Okanishi T., T. Matsui, T. Takeguchi, R. Kikuchi and K. Eguchi, 2006, “Chemical interaction between Pt and SnO<sub>2</sub> and influence on adsorptive properties of carbon monoxide”, *Applied Catalysis A: General*, Vol. 298, pp. 181-187.
- Ozawa M. and M. Kimura, 1990, “Effect of cerium addition on the thermal stability of gamma alumina support”, *Journal of Materials Science Letters*, Vol. 9, pp. 291-293.

- Panagiotopoulou P., J. Papavasiliou, G. Avgouropoulos, T. Ioannides and D. I. Kondarides, 2007, "Water-gas shift activity of doped Pt/CeO<sub>2</sub> catalysts", *Chemical Engineering Journal*, Vol. 134, pp. 16-22.
- Panagiotopoulou P., D.I. Kondarides, 2007, "A comparative study of the water gas shift activity of Pt catalysts supported on single (MO<sub>x</sub>) and composite (MO<sub>x</sub>/Al<sub>2</sub>O<sub>3</sub>, MO<sub>x</sub>/TiO<sub>2</sub>) metal oxide carriers, *Catalysis Today*, Vol. 127, pp. 319-329.
- Panagiotopoulou P. and D. I. Kondarides, 2006, "Effect of the nature of the support on the catalytic performance of noble metal catalysts for the water-gas shift reaction", *Catalysis Today*, Vol. 112, pp. 49-52.
- Panagiotopoulou P. and D. I. Kondarides, 2004, "Effect of morphological characteristics of TiO<sub>2</sub>-supported noble metal catalysts on their activity for the water-gas shift reaction", *Journal of Catalysis*, Vol. 225, pp. 327-336.
- Patel, S. and K. K. Pant, 2006, "Activity and Stability Enhancement of Copper-Alumina Catalysts Using Cerium and Zinc Promoters for the Selective Production of Hydrogen Via Steam Reforming of Methanol", *Journal of Power Sources*, Vol. 159, pp. 139-143.
- Pierre D., W. Deng and M. Flytzani-Stephanopoulos, 2007, "The Importance of Strongly Bound Pt-CeO<sub>x</sub> Species for the Water-gas Shift Reaction: Catalyst Activity and Stability Evaluation", *Topics in Catalysis*, Vol. 46, pp. 363-373.
- Qi A., B. Peppley and K. Karan, 2007, "Integrated fuel processors for fuel cell application: A review", *Fuel Processing Technology*, Vol. 88, pp. 3-22.
- Qi X. and M. Flytzani-Stephanopoulos, 2004, "Activity and stability of Cu-CeO<sub>2</sub> catalysts in high-temperature water-gas shift for fuel-cell applications", *Industrial and Engineering Chemistry Research*, Vol. 43, pp. 3055-3062.

- Radhakrishnan R., R. R. Willigan, Z. Dardas and T. H. Vanderspurt, 2006, "Water gas shift activity and kinetics of Pt/Re catalysts supported on ceria-zirconia oxides", *Applied Catalysis B: Environmental*, Vol. 66, pp. 23-28.
- Radhakrishnan R., R. R. Willigan, Z. Dardas and T. H. Vanderspurt, 2006, "Water Gas Shift Activity of Noble Metals Supported on Ceria-Zirconia Oxides", *AIChE Journal*, Vol. 52, pp. 1888-1894.
- Rangel M. D., R. M. Sasaki and F. Galenbeck, 1995, "Effect of chromium on magnetite formation", *Catalysis Letters*, Vol. 33, pp. 237-254.
- Reese M. A., S. Q. Turn and H. Cui, 2009, "High pressure autothermal reforming in low oxygen environments", *Journal of Power Sources*, Vol. 187, pp. 544-554.
- Rhodes C., B. P. Williams, F. King and G. J. Hutchings, 2002, "Promotion of  $\text{Fe}_3\text{O}_4/\text{Cr}_2\text{O}_3$  high temperature water gas shift catalyst", *Catalysis Communications*, Vol. 3, pp. 381-384.
- Ricote S., G. Jacobs, M. Milling, Y. Ji, P. M. Patterson and B. H. Davis, 2006, "Low temperature water-gas shift: Characterization and testing of binary mixed oxides of ceria and zirconia promoted with Pt", *Applied Catalysis A: General*, Vol. 303, pp. 35-47.
- Roth D., P. Gelina, E. Tenab and M. Primet, 2001, "Combustion of methane at low temperature over Pd and Pt catalysts supported on  $\text{Al}_2\text{O}_3$ ,  $\text{SnO}_2$  and  $\text{Al}_2\text{O}_3$ -grafted  $\text{SnO}_2$ ", *Topics in Catalysis*, Vol. 16/17, pp. 77-82.
- Ruettinger, W., O. Ilinich and R. J. Farrauto, 2003, "A New Generation of Water Gas Shift Catalysts for Fuel Cell Applications", *Journal of Power Sources*, Vol. 118, pp. 61-65.
- Sato Y., Y. Soma, T. Miyao and S. Naito, 2006, "The water-gas-shift reaction over Ir/ $\text{TiO}_2$  and Ir-Re/ $\text{TiO}_2$  catalysts", *Applied Catalysis A: General*, Vol. 304, pp. 78-85.

- Scott L.S., M.M. Seahaug, C.T. Holt and W.J. Dawson, 2001, "Fuel processing catalysts based on nanoscale ceria", *Fuel Cells Bulletin*, Vol. 4, pp. 7-10.
- Sedmak, G., S. Hocevar and J. Levec, 2004, "Transient Kinetic Model of CO Oxidation over Nanostructured  $\text{Cu}_{0.1}\text{Ce}_{0.9}\text{O}_{2-y}$  Catalyst", *Journal of Catalysis*, Vol. 222, pp. 87-99.
- Sekine Y., H. Takamatsu, S. Aramaki, K. Ichishima, M. Takada, M. Matsukata and E. Kikuchi, 2009, "Synergistic effect of Pt or Pd and perovskite oxide for water gas shift reaction" *Applied Catalysis A: General*, Vol. 352, pp. 214-222.
- Semelsberger T. A., L. F. Brown, R. L. Borup and M. A., 2004, "Inbody Equilibrium products from autothermal processes for generating hydrogen-rich fuel-cell feeds", *International Journal of Hydrogen Energy*, Vol. 29, pp. 1047-1064.
- Shamsi A., 2009, "Partial oxidation of methane and the effect of sulfur on catalytic activity and selectivity", *Catalysis Today*, Vol. 139, pp. 268-273.
- Shishido T., S. Nishimura, Y. Yoshinaga, K. Ebitani, K. Teramura and T. Tanaka, 2009, "High sustainability of Cu–Al–Ox catalysts against daily start-up and shut-down (DSS)-like operation in the water–gas shift reaction", *Catalysis Communications* Vol.10, pp. 1057-1061.
- Shishido T., M.Yamamoto, I. Atake, D. Li, Y. Tian, H. Morioka, M. Honda, T. Sano and K. Takehira, 2006, "Cu/Zn-based catalysts improved by adding magnesium for water–gas shift reaction", *Journal of Molecular Catalysis A: Chemical* Vol. 253, pp. 270-278.
- Solieman A. A. A., J. W. Dijkstra, W. G. Haije, P. D. Cobden and R.W. Brink, 2009, "Calcium oxide for CO<sub>2</sub> capture: Operational window and efficiency penalty in sorption-enhanced steam methane reforming", *International Journal of Greenhouse Gas Control*, In press.

- Song, C., 2002, "Fuel Processing for Low-Temperature and High-Temperature Fuel Cells: Challenges and Opportunities for Sustainable Development in the 21<sup>st</sup> Century", *Catalysis Today*, Vol. 77, pp. 17-49.
- Sun W. Z., G. Q. Jin and X. Y. Guo, 2005, Partial oxidation of methane to syngas over Ni/SiC catalysts, *Catalysis Communications*, Vol. 6, pp. 135-139.
- Şen, Ö., 2008, "Construction and Testing of a Low-Temperature Water-Gas Shift Reaction System", M. S. Thesis, Boğaziçi University, Istanbul.
- Tabakova T., V. Idakiev, J. Papavasiliou, G. Avgouropoulos and T. Ioannides, 2007, "Effect of additives on the WGS activity of combustion synthesized CuO/CeO<sub>2</sub> catalysts", *Catalysis Communications*, Vol. 8, pp. 101-106.
- Tanaka Y., T. Takeguchi, R. Kikuchi and K. Eguchi, 2005, "Influence of preparation method and additive for Cu–Mn spinel oxide catalyst on water gas shift reaction of reformed fuels", *Applied Catalysis A: General*, Vol. 279, pp. 59-66.
- Tanaka Y., T. Utaka, R. Kikuchi, K. Sasaki and K. Eguchi, 2003a, "Water gas shift reaction over Cu-based mixed oxides for CO removal from the reformed fuels", *Applied Catalysis A: General*, Vol. 242, pp. 287–295.
- Tanaka Y., T. Utaka, R. Kikuchi, T. Takeguchi, K. Sasaki, and K. Eguchi, 2003b, "Water gas shift reaction for the reformed fuels over Cu/MnO catalysts prepared via spinel-type oxide", *Journal of Catalysis*, Vol. 215, pp. 271-278.
- Thinon O., F. Diehl, P. Avenier and Y. Schuurman, 2008, "Screening of bifunctional water-gas shift catalysts", *Catalysis Today*, Vol.137, pp. 29–35.
- Trimm D. L., 2005, "Minimisation of carbon monoxide in a hydrogen stream for fuel cell application", *Applied Catalysis A: General*, Vol. 296, pp. 1-11.

- Trovarelli A., M. Boaro, E. Rocchini, C. Leitenburg and G. Dolcetti, 2001, "Some recent developments in the characterization of ceria-based catalysts", *Journal of Alloys and Compounds*, Vol. 323–324, pp. 584-591.
- Twigg M.V. (editor), 1989, *Catalyst Handbook, Chapter 6: 'Water-gas shift'*, 2nd ed., Wolfe Press, London.
- Utaka T., K. Sekizawa and K. Eguchi, 2000, "CO removal by oxygen-assisted water gas shift reaction over supported Cu catalysts", *Applied Catalysis A: General*, Vol. 194/195, pp. 21-26.
- Wang X., R. J. Gorte and J. P. Wagner, 2002, "Deactivation Mechanisms for Pd/Ceria during the Water–Gas-Shift Reaction", *Journal of Catalysis*, Vol. 212, pp. 225-230.
- Wen, W., L. Jing, M. G. White, N. Marinkovic, J. C. Hanson and J. A. Rodriguez, 2007, "In Situ Time-Resolved Characterization of Novel Cu-MoO<sub>2</sub> Catalysts during the Water-Gas Shift Reaction", *Catalysis Letters*, Vol. 113, pp. 1-6.
- Whittington B. I., C. J. Jiang and D. L. Trimm, 1995, "Vehicle exhaust catalysis: I. The relative importance of catalytic oxidation, steam reforming and water-gas shift reactions", *Catalysis Today*, Vol. 26, pp. 41-45.
- Xua D., P. Daib, X. Liua, C. Caoa and Q. Guoa, 2008, "Carbon-supported cobalt catalyst for hydrogen generation from alkaline sodium borohydride solution" *Journal of Power Sources*, Vol.182, pp. 616-620
- Yahiro H., K. Murawaki, K. Saiki, T. Yamamoto and H.Yamaura, 2007, "Study on the supported Cu-based catalysts for the low-temperature water–gas shift reaction", *Catalysis Today*, Vol. 126, pp. 436-440.
- Yeragi, D. C., N. C. Pradhan and A. K. Dalai, 2006, "Low-Temperature Water-Gas Shift Reaction over Mn-Promoted Cu/Al<sub>2</sub>O<sub>3</sub> Catalysts", *Catalysis Letters*, Vol. 112, pp. 139-148.

Zalc, J. M. and D. G. Löffler, 2002, "Fuel Processing for PEM Fuel Cells: Transport and Kinetic Issues of System Design", *Journal of Power Sources*, Vol. 111, pp. 58-64.

Zalc J. M., V. Sokolovskii and D. G. Löfler, 2002, "Are Noble Metal-Based Water-Gas Shift Catalysts Practical for Automotive Fuel Processing?", *Journal of Catalysis*, Vol. 206, pp. 169-171.

Zerva C. and C. J. Philippopoulos, 2006, "Ceria catalysts for water gas shift reaction: Influence of preparation method on their activity", *Applied Catalysis B: Environmental*, Vol. 67, pp. 105-112.